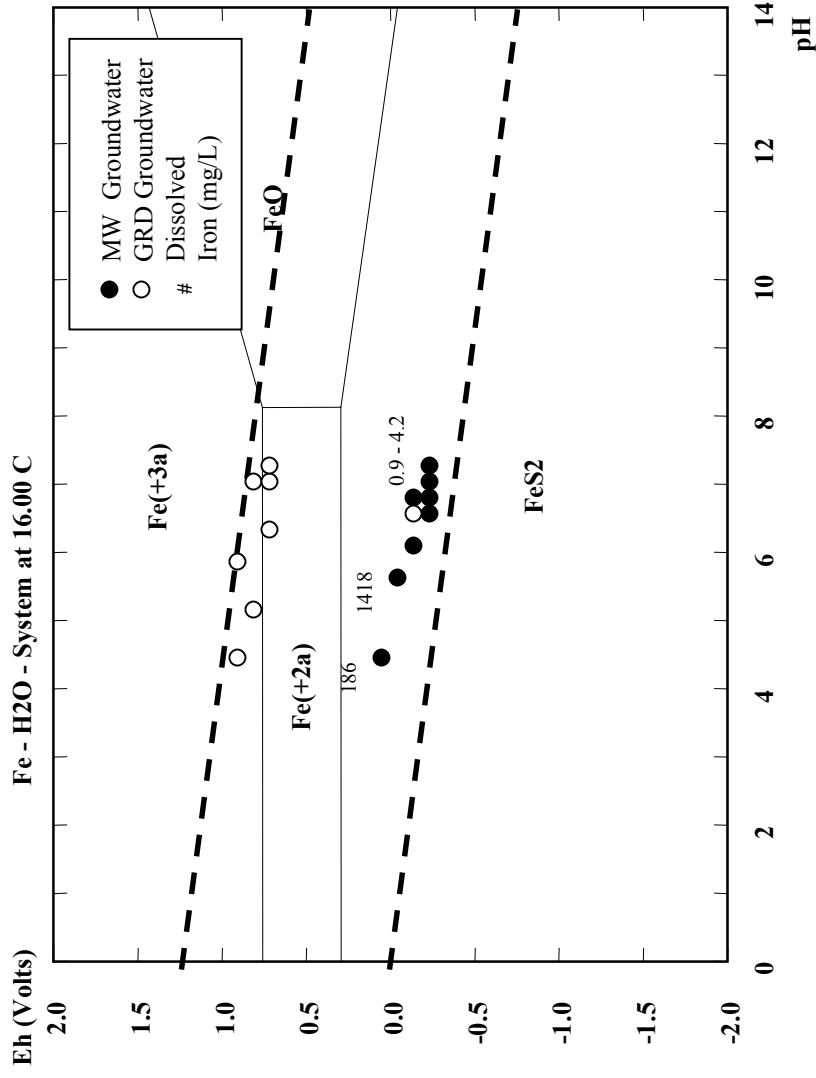
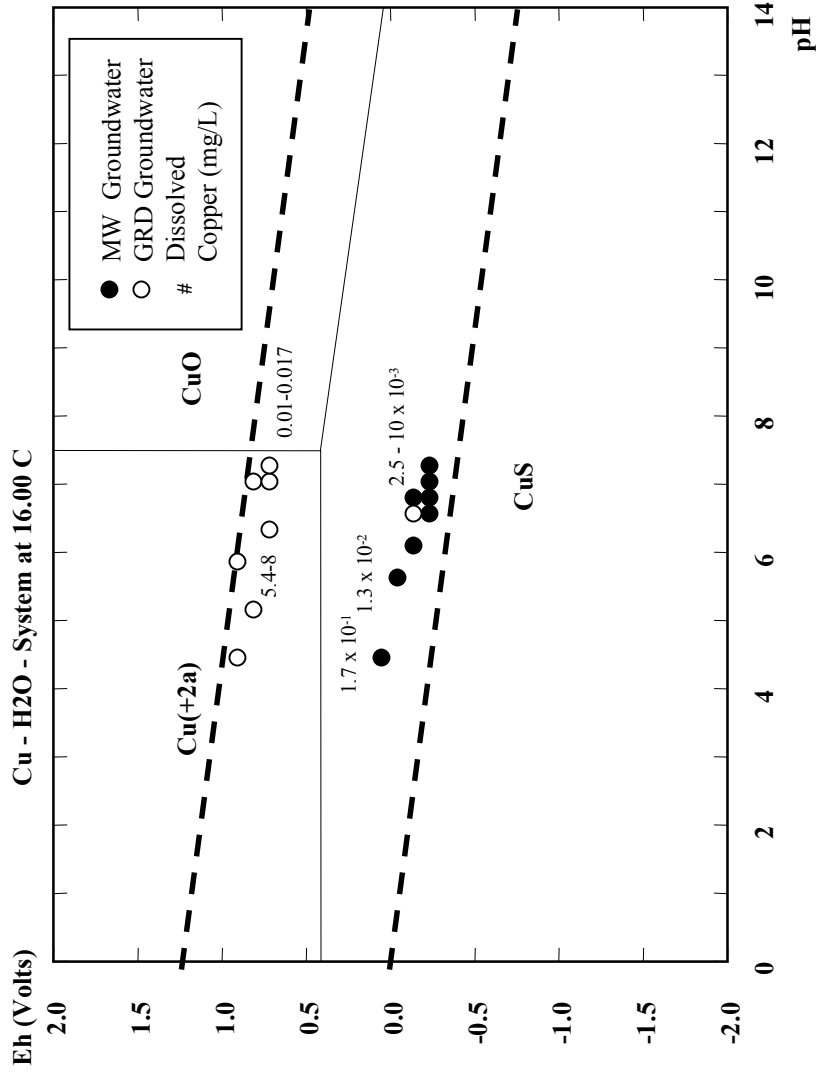


**Figure E-1-1** Eh-pH diagram for the System S-O-H From Monitoring Well and Surface Samples Collected 11/01. Heavy dashed lines represent stability field of water and solid lines represent dominant fields for aqueous (or solid sulfur) species for a total sulfur concentration of  $2.3 \times 10^{-3}$  M (MW 20).



**Figure E-1 -2** Eh-pH diagram for the System Fe-S-O-H From Monitoring Well and Surface Samples Collected 11/01. Heavy dashed lines represent stability field of water and solid lines represent dominant fields for aqueous species for a total iron concentration of  $3.4 \times 10^{-5}$  M (MW 20).



**Figure E-1 -3** Eh-pH diagram for the System Cu-S-O-H From Monitoring Well and Surface Samples Collected 11/01. Heavy dashed lines represent stability field of water and solid lines represent dominant fields for aqueous species for a total copper concentration of  $1.0 \times 10^{-7}$  M (MW 20).

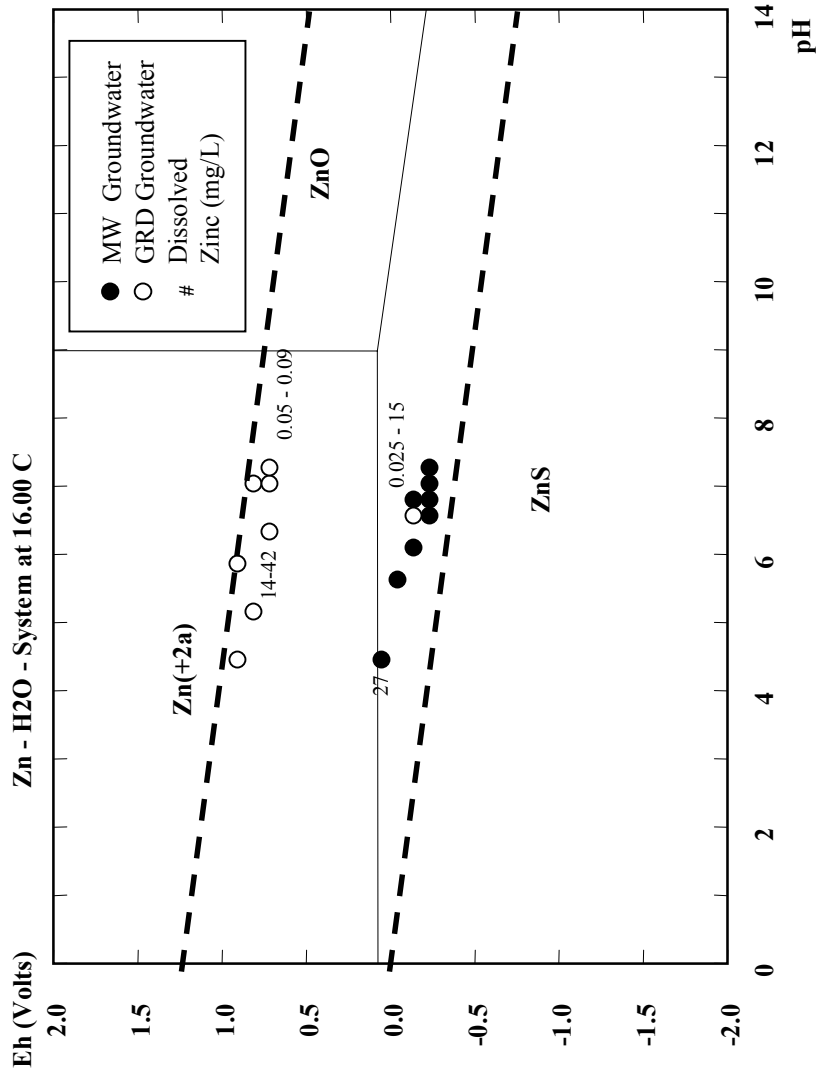


**Figure E-1-4** Eh-pH diagram for the System Zn-S-O-H From Monitoring Well and Surface Samples Collected 11/01. Heavy dashed lines represent stability field of water and solid lines represent dominant fields for aqueous species for a total zinc concentration of  $4.7 \times 10^{-7}$  M (MW 20)

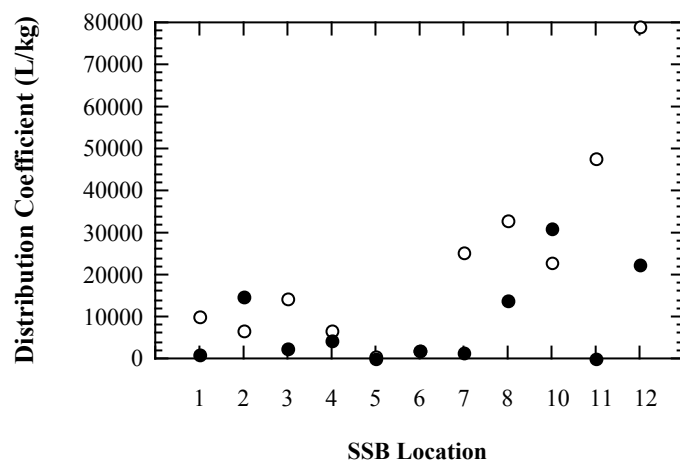


**Figure E-1-5** Measured distribution coefficients in SSB Wells

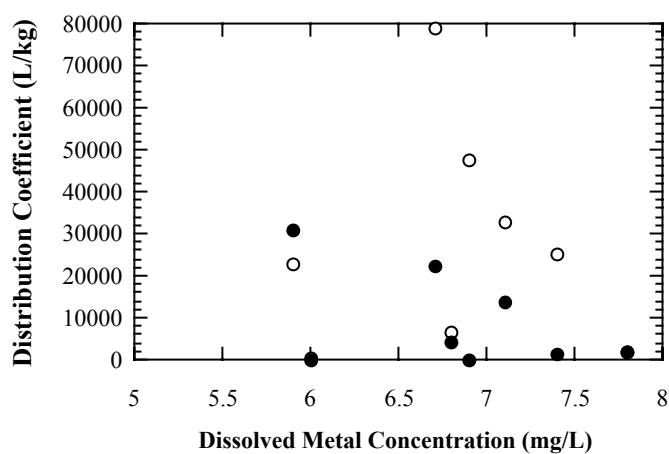
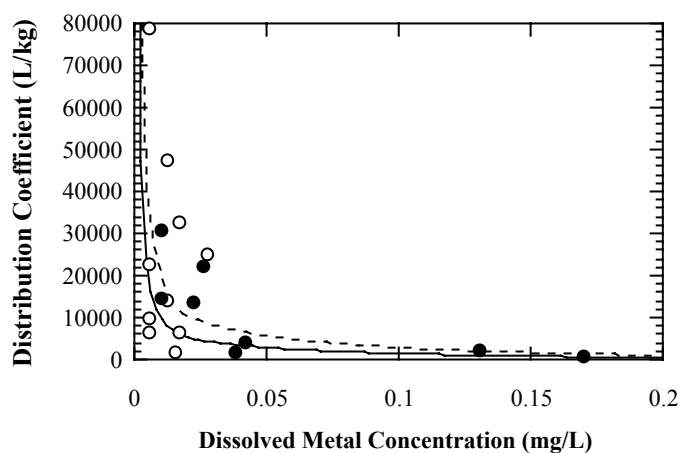
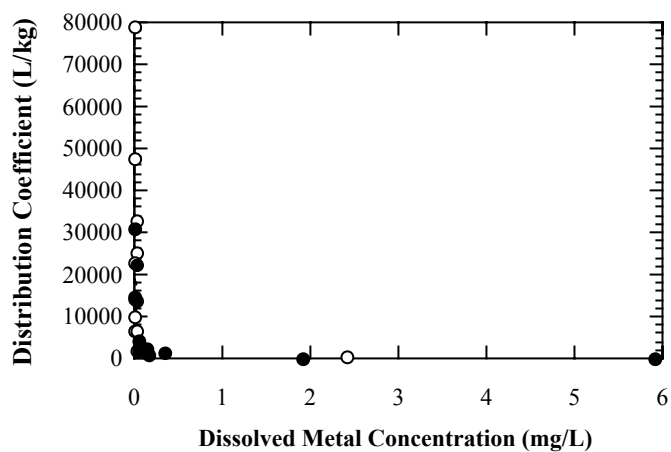


**Figure E-1-7** Measured distribution coefficients versus dissolved concentrations in SSB Wells (Copper = open circles; Zinc = closed circles). (a) Trends for aqueous phase dependence (Copper = solid lines; Zinc = dashed lines); (b) Trends for aqueous phase dependence (zoomed in); (c) pH dependence (see text).

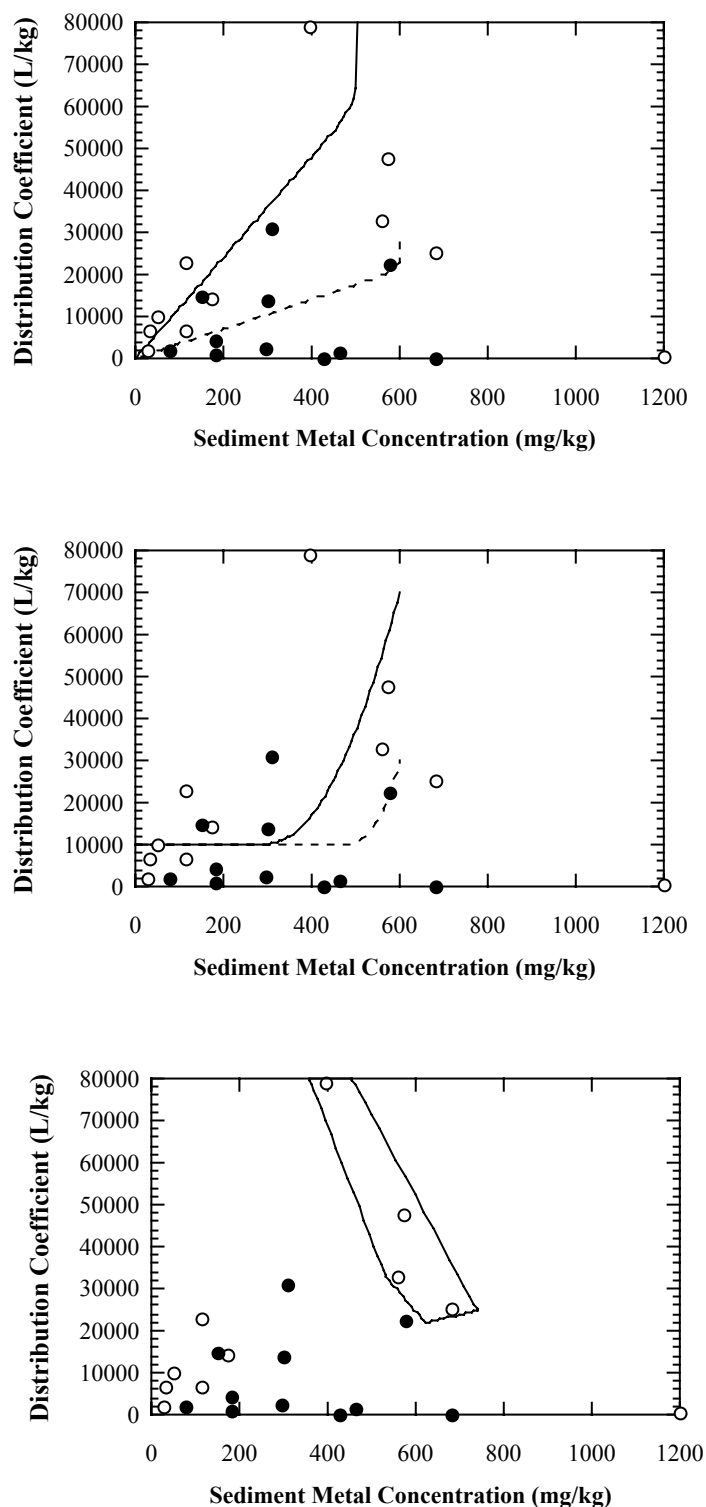


**Figure E-1-6** Measured distribution coefficients versus sediment concentrations in SSB Wells (Copper = open circles; Zinc = closed circles). (a) Trends for reaching sorption capacity (Copper = solid lines; Zinc = dashed lines). ; (b) Trends for precipitation at higher concentrations; (c) Trends if biased by sulfide phases(see text).

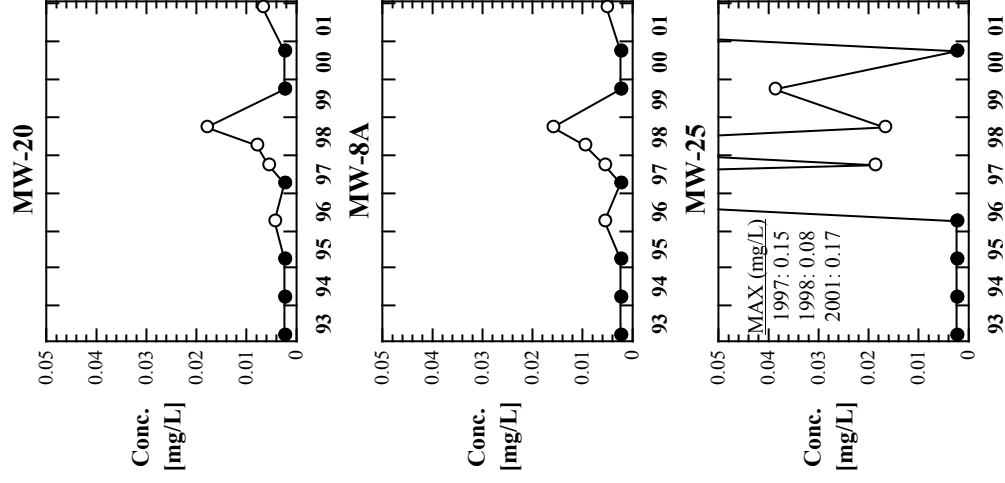


**FIGURE E-1-8a** Summary of Monitoring Well Copper Concentrations for the Period 1993-2001 (Solid Circles are Detection Limit and Empty Circles are Measured Values)

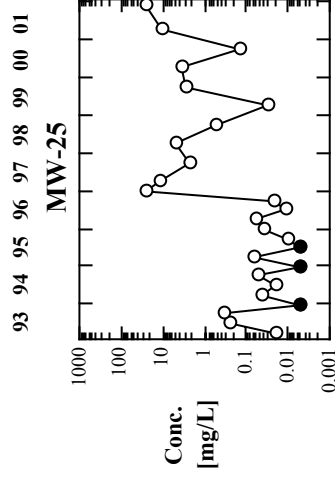
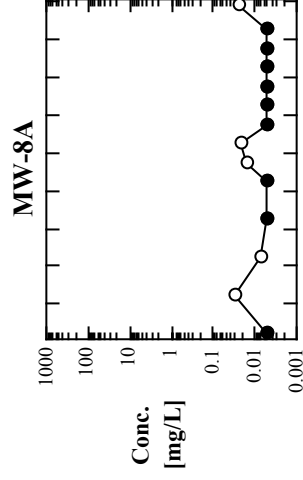
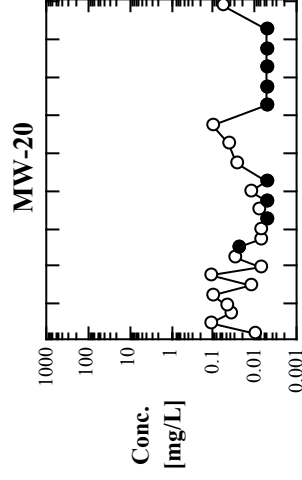
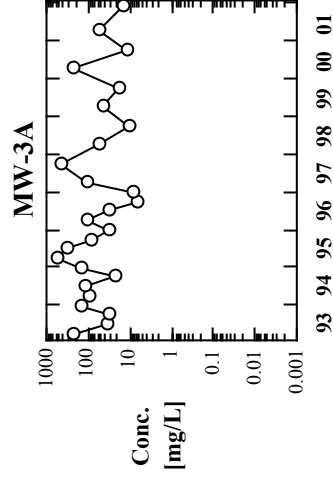
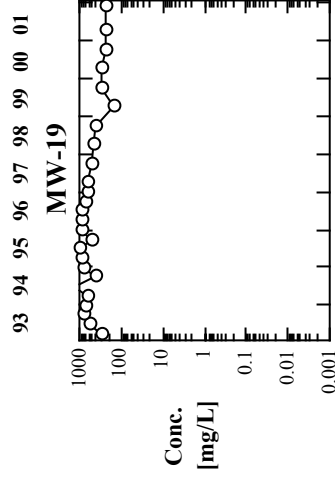
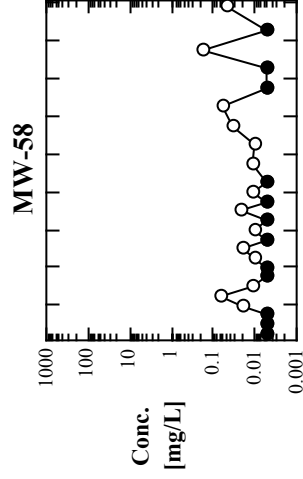
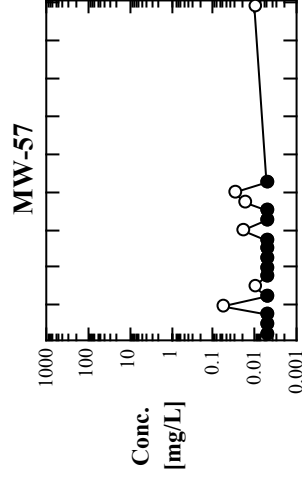
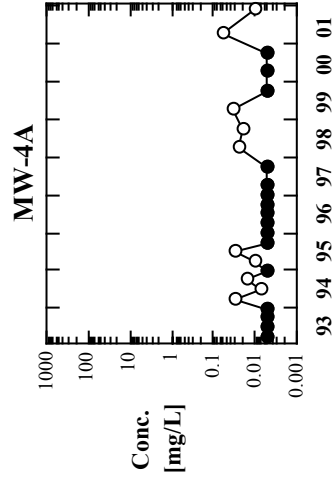
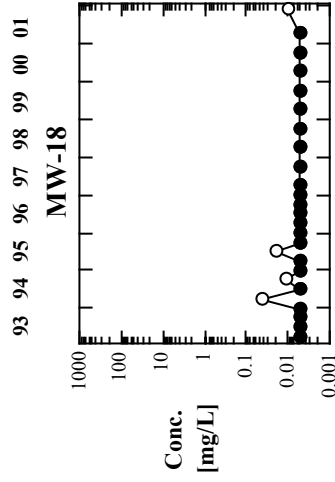
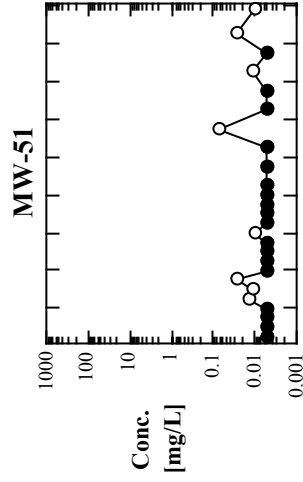
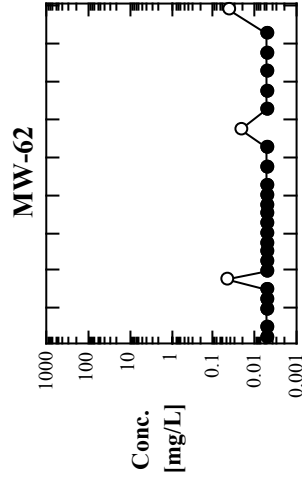


**FIGURE E-1-8b** Summary of Monitoring Well Zinc Concentrations for the Period 1993-2001 (Solid Circles are Detection Limit and Empty Circles are Measured Values)

**TABLE E-1-1 Measured Groundwater Chemistry of Shallow Wells**

LOCATION	WELL NAME AND NUMBER	DATE	DEPTH (ft)	pH	Hardness (mg/L)	TOC/TSS <sup>4</sup>	Dissolved Sulfide (mg/L)	Sulfate (mg/L)	Total Copper (mg/L)	Dissolved Copper (mg/L)	Copper Kd (L/kg)	Total Zinc (mg/L)	Dissolved Zinc (mg/L)	Zinc Kd (L/kg)
NORTH	SSB1	7/25/01	0-0.5	6.9					0.005		10,000	0.170		1,059
	SSB2	7/25/01	0-0.5	7.0					0.005		6,800	0.010		15,000
	SSB3	7/25/01	1-1.5	6.4					0.012		14,417	0.130		2,277
	GRD1	11/14/01		7.1	4900	0.03	<0.04	970	0.016 J	0.017 J <sup>1</sup>		<0.050	0.088	
	GRD2	11/14/01		6.9	2600	0.01	<0.04	350	0.008 J	0.011 J <sup>1</sup>		<0.050	<0.050	
	GRD3	11/14/01		6.7	3300	0.01	<0.04	8	<0.005 UJ	0.010 J <sup>1</sup>		<0.050	<0.050	
	Average			6.8			<0.04	443	0.009	0.013	10,406	0.077	0.063	6,112
	Median			6.9			<0.04	350	0.007	0.011	10,000	0.050	0.050	2,277
SOUTH	SSB4	7/19/01	1-1.5	6.8					0.017		6,765	0.042		4,310
	SSB5	7/19/01	4-4.5	6.0					2.400		500	5.900		115
	SSB6	7/25/01	1-1.5	7.8					0.015		1,867	0.038		2,079
	SSB7	7/19/01	4-4.5	7.4					0.027		25,185	0.350		1,329
	SSB8	7/19/01	0-0.5	7.1					0.017		32,941	0.022		13,636
	SSB10	7/25/01	4-4.5	5.9					0.005		22,800	0.010		31,100
	SSB11	7/25/01	3-3.5	6.9					0.012		47,667	1.900		226
	SSB12	7/19/01	0-0.5	6.7					0.005		79,000	0.026		22,192
	GRD4	11/14/01		6.9	7000	0.14	69	130	0.008 J <sup>1</sup>	0.009 J <sup>1</sup>		<0.050	<0.050	
	GRD5	11/14/01		4.8	2700	0.02	<0.04	1800	8.800 J <sup>1</sup>	9.300 J <sup>1</sup>		22.000	25.000	
	GRD6	11/14/01		5.5	2500	0.50	<0.04	1300	6.000 J <sup>1</sup>	5.400 J <sup>1</sup>		21.000	18.000	
	GRD7	11/14/01		4.2	720	1.00	<0.04	600	8.200 J <sup>1</sup>	7.800 J <sup>1</sup>		16.000	14.000	
	GRD8	11/14/01		6.2	1200	0.13	<0.04	1200	9.100 J <sup>1</sup>	8.000 J <sup>1</sup>		35.000	42.000	
	Average			6.3			<0.04	1006	2.662	6.102	27,091	7.872	19.810	9,373
	Median			6.7			<0.04	1200	0.017	7.8	23,993	0.350	18.000	3,194
SF BAY	RMP <sup>2</sup>			7.7						0.002	33507		0.001	351586
	WQO <sup>3</sup>										0.031		0.081	

<sup>1</sup>J indicates an estimated value; <sup>2</sup>Based on average values of nearby RMP Stations (Pacheco Creek, Grizzly Bay, Honker Bay (SFEI, 1994-1999);

<sup>3</sup>Ambient Bay Water Quality Objectives are 0.0031 mg/L for Copper and 0.081 mg/L for Zinc (California Toxics Rule, EPA (2000)) (Shading indicates higher concentrations)

<sup>4</sup>TOC/TSS is a relative indicator of dissolved organic matter if TOC/DOC ratio is relatively constant; Higher values in southern spread may indicate higher DOC

**TABLE E-1-2 Predicted Copper and Zinc Speciation in Shallow Wells**

PARAMETER	GRD 5			GRD 1		
Conventional	<b>T:</b>	16	(deg. C)	<b>T:</b>	16	(deg. C)
	<b>pH:</b>	4.8		<b>pH:</b>	7.1	
	<b>Eh:</b>	1.0		<b>Eh:</b>	0.8	
	<b>Salinity:</b>	1.5	(ppt)	<b>Salinity:</b>	2.8	ppt
	<b>Hardness:</b>	2700	(mg/L as CaCO3)	<b>Hardness:</b>	4900	(mg/L as CaCO3)
Dissolved Concentrations	<b>Copper:</b>	<b>9.354</b>	(mg/L)	<b>Copper:</b>	<b>0.017</b>	(mg/L)
	<i>CuHCO3+</i>	3.682	(mg/L)	<i>Cu(L2)</i>	0.014	(mg/L)
	<i>Cu(L2)</i>	3.315	(mg/L)	<i>Cu(L1)</i>	0.003	(mg/L)
	<i>Cu+2</i>	1.347	(mg/L)			(mg/L)
	<b>Zinc:</b>	<b>25.148</b>	(mg/L)	<b>Zinc:</b>	<b>0.050</b>	(mg/L)
	<i>Zn(L2)</i>	9.740	(mg/L)	<i>Zn(L2)</i>	0.043	(mg/L)
	<i>Zn+2</i>	5.973	(mg/L)	<i>Zn(L1)</i>	0.008	(mg/L)
	<i>ZnHCO3+</i>	5.422	(mg/L)			
Saturation State of Important Phases	<b>Gypsum</b>	0.0	S.I.	<b>Gypsum</b>	-0.1	S.I.
	<b>Calcite</b>	-1.3	S.I.	<b>Calcite</b>	1.5	S.I.
	<b>Jarosite</b>	5.0	S.I.	<b>Jarosite</b>	4.3	S.I.
	<b>Ferrihydrite</b>	-0.4	S.I.	<b>Ferrihydrite</b>	1.9	S.I.
	<b>Lepidocrocite</b>	3.2	S.I.	<b>Lepidocrocite</b>	5.4	S.I.
	<b>Cupric Ferrite</b>	6.7	S.I.	<b>Cupric Ferrite</b>	6.0	S.I.
	<b>Cu(OH)2</b>	-4.6	S.I.	<b>Cu(OH)2</b>	-9.9	S.I.
	<b>Tenorite</b>	-3.6	S.I.	<b>Tenorite</b>	-8.8	S.I.
	<b>Zincite</b>	-6.5	S.I.	<b>Zincite</b>	-11.8	S.I.
	<b>Zn(OH)2</b>	-6.4	S.I.	<b>Zn(OH)2</b>	-11.6	S.I.
Predicted Dissolved Concentrations	<b>Sorbed Equilibrium</b>			<b>Sorbed Equilibrium</b>		
	<b>Copper</b>	<b>4.303</b>	(mg/L)	<b>Copper</b>	<b>0.017</b>	(mg/L)
	<b>Zinc</b>	<b>11.505</b>	(mg/L)	<b>Zinc</b>	<b>0.050</b>	(mg/L)
	<b>Mineral Equilibrium<sup>1,4</sup></b>			<b>Mineral Equilibrium<sup>2,4</sup></b>		
	<b>Copper</b>	<b>9.195</b>	(mg/L)	<b>Copper</b>	<b>0.017</b>	(mg/L)
	<b>Zinc</b>	<b>25.148</b>	(mg/L)	<b>Zinc</b>	<b>0.050</b>	(mg/L)

<sup>1</sup>Precipitated phases are Cupric Ferrite and Gypsum; <sup>2</sup>Precipitated phase are Lepidocrocite and Calcite; <sup>3</sup>Precipitated phase is Cupric Ferrite;

<sup>4</sup>Dissolution allowed with respect to Montmorillonite but no change found in solution pH

**TABLE E-1-3 Measured Groundwater Chemistry of Deep Wells**

LOCATION	WELL NAME AND NUMBER	DATE	DEPTH	pH	Average pH <sup>1</sup>	Median pH <sup>1</sup>	Dissolved Sulfide (mg/L)	Dissolved Sulfate (mg/L)	Average Dissolved Copper (mg/L) <sup>1</sup>	Median Dissolved Copper (mg/L) <sup>1</sup>	Average Dissolved Zinc (mg/L) <sup>1</sup>	Median Dissolved Zinc (mg/L) <sup>1</sup>
NORTH	MW62	11/12/01	18-20.5	6.8	6.9	6.9	R	<0.50	0.005	0.003	0.009	0.005
	MW51	11/12/01	15-20	7.1	7.3	7.4	R	12	0.005	0.003	0.011	0.005
	MW18	11/12/01	7.5-12.5	7.1	7.2	7.2	0.05	5.0	0.005	0.003	0.007	0.005
	MW4A	11/12/01	8.5-18.5	7.0	7.1	7.2	17	30	0.005	0.003	0.012	0.005
SOUTH	MW57	11/12/01	10-20	7.4	6.9	7.0	R	1200	0.003	0.003	0.012	0.005
	MW58	11/12/01	10-20	7.0	6.8	6.8	R	4.3	0.007	0.003	0.023	0.010
	MW19	11/14/01	9.5-15.5	5.8	5.5	5.6	<0.04	9,700	0.003	0.003	593.590	627.500
	MW3A	11/14/01	4.5-14.5	6.3	6.1	6.2	<0.04	6,800	0.248	0.003	118.846	57.500
	MW20	11/14/01	7.5-12.5	6.7	6.7	6.8	11	190	0.005	0.003	0.032	0.012
	MW8A	11/14/01	8.5-18.5	7.0	6.8	6.9	23	34	0.005	0.003	0.011	0.005
	MW8Ad	11/14/01	8.5-18.5	7.0			18	32				
	MW25	11/14/01	4.5-7	4.5	5.4	6.1	<0.04	5,000	0.045	0.017	3.504	0.066
SF BAY	RMP <sup>2</sup>				7.7				0.002		0.001	
	WQO <sup>3</sup>								0.031		0.081	

<sup>1</sup> Average and median values for the period 1993-2001; <sup>2</sup>Based on average values of nearby RMP Stations (Pacheco Creek, Grizzly Bay, Honker Bay (SFEI, 1994-1999);

<sup>3</sup>Ambient Bay Water Quality Objectives are 0.0031 mg/L for Copper and 0.081 mg/L for Zinc (California Toxics Rule, EPA (2000)) (Shading indicates higher concentrations)

**TABLE E-1-4 Predicted Copper and Zinc Speciation in Deep Wells**

PARAMETER	MW 25			MW 20		
<b>Conventionals</b>	<b>T:</b>	16	(deg. C)	<b>T:</b>	16	(deg. C)
	<b>pH:</b>	4.5		<b>pH:</b>	6.7	
	<b>Eh:</b>	0.0		<b>Eh:</b>	-0.2	
	<b>Salinity:</b>	2.1	(ppt)	<b>Salinity:</b>	1.7	ppt
	<b>Hardness:</b>	6500	(mg/L as CaCO3)	<b>Hardness:</b>	3300	(mg/L as CaCO3)
<b>Dissolved Concentrations</b>	<b>Copper:</b>	<b>0.172</b>	(mg/L)	<b>Copper:</b>	<b>0.007</b>	(mg/L)
	<i>CuCl2-</i>	<i>0.112</i>	(mg/L)	<i>Cu(HS)</i>	<i>0.007</i>	(mg/L)
	<i>Cu(HS)</i>	<i>0.040</i>	(mg/L)			(mg/L)
	<i>CuCl3-2</i>	<i>0.018</i>	(mg/L)			(mg/L)
	<b>Zinc:</b>	<b>27.364</b>	(mg/L)	<b>Zinc:</b>	<b>0.057</b>	(mg/L)
	<i>Zn+2</i>	<i>26.952</i>	(mg/L)	<i>Zn(HS)2</i>	<i>0.047</i>	(mg/L)
	<i>ZnCl+</i>	<i>0.257</i>	(mg/L)	<i>Zn(L1)</i>	<i>0.008</i>	(mg/L)
	<i>ZnHCO3+</i>	<i>0.071</i>	(mg/L)	<i>Zn(L2)</i>	<i>0.002</i>	(mg/L)
<b>Saturation State of Important Phases</b>	<b>Chalcocite</b>	10.0	S.I.	<b>Chalcocite</b>	-1.8	S.I.
	<b>Covellite</b>	3.8	S.I.	<b>Covellite</b>	0.4	S.I.
	<b>Pyrite</b>	1.0	S.I.	<b>Pyrite</b>	1.0	S.I.
	<b>Sulfur</b>	-6.4	S.I.	<b>Sulfur</b>	-1.5	S.I.
	<b>Sphalerite</b>	-1.7	S.I.	<b>Sphalerite</b>	1.5	S.I.
<b>Predicted Dissolved Concentrations</b>	<b>Sorbed Equilibrium<sup>1</sup></b>			<b>Sorbed Equilibrium<sup>3</sup></b>		
	<b>Copper</b>	<b>0.172</b>	(mg/L)	<b>Copper</b>	<b>0.007</b>	(mg/L)
	<b>Zinc</b>	<b>19.454</b>	(mg/L)	<b>Zinc</b>	<b>0.057</b>	(mg/L)
	<b>Mineral Equilibrium<sup>2</sup></b>			<b>Mineral Equilibrium<sup>4</sup></b>		
	<b>Copper</b>	<b>0.0001</b>	(mg/L)	<b>Copper</b>	<b>0.003</b>	(mg/L)
	<b>Zinc</b>	<b>27.364</b>	(mg/L)	<b>Zinc</b>	<b>0.002</b>	(mg/L)

<sup>1</sup>If Cu(II) reduction is kinetically inhibited then sorbed equilibria is 0.032 mg/L; <sup>2</sup>Precipitated phases are Chalcocite and Pyrite;

<sup>3</sup>If Cu(II) reduction is kinetically inhibited then sorbed equilibria is 0.007 mg/L; <sup>4</sup>Precipitated phases are Covellite, Pyrite, and Sphalerite

**Table E-1-5 Summary of Sulfate Reduction and Metal Precipitation Rates at Ambient Conditions**

Element	Reaction	Rate (mg/yr)	Condition	Reference
Sulfur	$\text{SO}_4^{2-} + 2 \text{H}^+ = \text{H}_2\text{S} + 2 \text{O}_2$	1.8E-01 1.0E-07 9.0E-17	Inorganic; pH = 2; $\Sigma\text{S}_{\text{tot}} = 0.01 \text{ mol}$ Inorganic; pH = 4-7; $\Sigma\text{S}_{\text{tot}} = 0.01 \text{ mol}$ Inorganic; pH = 9; $\Sigma\text{S}_{\text{tot}} = 0.01 \text{ mol}$	Ohmoto and Lasaga (1982)
	$\text{CH}_2\text{O} + 0.5 \text{SO}_4^{2-} + \text{H}^+ = 0.5 \text{H}_2\text{S} + \text{CO}_2 + \text{H}_2\text{O}$	5-450 2200 6000 23000	Sandy Aquifer; TOC = 0.01 wt % Marine Sediments Mining Lake Simulated Wetland; Nutrient Spike	Jakobsen and Postma (1999) Boudreau and Canfield (1984) Blodau et al. (1998) Reynolds et al. (1997)
Iron	$0.25 \text{CH}_2\text{O} + \text{FeOOH}(\text{S}) + 2 \text{H}^+ = 0.25 \text{CO}_2 + 1.75 \text{H}_2\text{O} + \text{Fe}^{2+}$	90 1300-4000	Sandy Aquifer; TOC = 0.01 wt % Mining Lake; Estimated	Jakobsen and Postma (1999) Blodau et al. (1998)
	$\text{Fe}^{2+} + \text{H}_2\text{S} = \text{FeS} + 2 \text{H}^+$	30 2.8E+06	Simulated Wetland; FeS Assumed; Cum. Rate Inorganic; Assumed $\Sigma\text{S}_{\text{tot}} = 0.001 \text{ mol}$	Reynolds et al. (1997) Rickard (1995)
Copper	$\text{Cu}^{2+} + \text{H}_2\text{S} = \text{CuS} + 2 \text{H}^+$	1.7E+08	Inorganic; pH = 2.0	Oktabybas et al. (1994)
Zinc	$\text{Zn}^{2+} + \text{H}_2\text{S} = \text{ZnS} + 2 \text{H}^+$	1.3 2.7E+07	Simulated Wetland; ZnS Assumed; Cum. Rate Inorganic; $\Sigma\text{S}_{\text{tot}} = 0.001 \text{ mol}$ ; Zn = 0.01 mol	Reynolds et al. (1997) Mishra and Das (1992)

## Appendix E-1 Contaminant Transport Processes

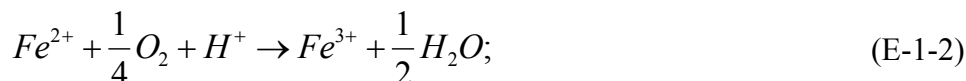
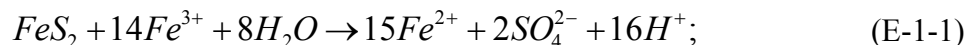
### E-1.1 Introduction

The important chemical processes affecting metal mobility at the project site are described in this section. Shallow and deep groundwater are discussed separately to emphasize the difference between metal transport in oxic and anoxic environments. Adsorption and precipitation are also distinguished as the two principal metal attenuation mechanisms leading to reduced dissolved metal concentrations in the groundwater. Conclusions include a discussion of current and projected groundwater metal concentrations, and inputs to the groundwater model of Section 3.5.6.

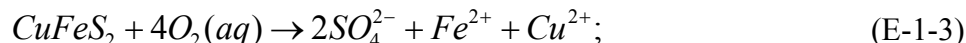
### E-1.2 Shallow Groundwater Transport

#### Introduction

There are two distinct geochemical zones of metal transport at the project site. The first is a near-surface zone, defined by the active microbiological reduction of organic carbon by aerobic bacteria. This zone is the principal source of dissolved metals and acid to groundwater. Based on AVS and acid generating potential measurements that identify remnant sulfides in the dredged spoil piles, acidity is likely generated by the following coupled reactions:



(Xu et al, 2000; Nordstrom and Alpers, 1999), where pyritic sulfide is oxidized by  $Fe^{+3}$  and reduced  $Fe^{+2}$  is subsequently oxidized by porewater oxygen. Depending on the nature of the copper and zinc sulfides remaining in the dredged spoil piles, elevated dissolved metal concentrations are likely produced by the following oxidation reactions:



and



where dissolved species are predicted to occur rather than oxidized metal carbonate, hydroxide, or oxide solid phases due to the low pH groundwater that results from the oxidation of pyrite (Blowes and Jambor, 1990).

#### Summary of Field Data

Near-surface groundwater and co-located sediment samples were collected at twelve SSB locations between the existing slough and realignment. These wells were screened at intervals ranging from 0.5 to 4.5 feet below the ground surface (Table E-1-1). Additional groundwater

samples were obtained from eight guard well (GRD) locations. The GRD wells were screened to collect both shallow and deep groundwater.

As shown in Table E-1-1, groundwater north of the tide gate is less variable than the southern spread area. All solutions north of the tide gate are close to neutrality, with an average pH of 6.8. Solutions are also oxidizing with respect to sulfur, evidenced by the lack of measured sulfide in the samples. Using measured pH and dissolved oxygen concentrations in the groundwater, and assuming equilibrium between aqueous and gaseous oxygen, the electropotential of eight GRD samples was calculated using the Nernst equation:

$$Eh = E^0 + \frac{2.303RT}{nF} \log \left( \frac{a_{O2(aq)}}{f_{O2(g)}} \right); \quad (E-1-5)$$

where  $R$  is the gas constant,  $F$  is the Faraday constant,  $T$  is the absolute temperature, and  $a$  is the activity of the specified aqueous species ( $f_{O2(g)} = 1.0$ ). Calculated redox states are presented as white circles on Figure E-1-1. Samples north of the tide gate cluster near neutrality in the stability field of sulfate. This is in contrast to samples from the southern spread area, where pH is as low as 4.2 (GRD 7) and can be reducing (GRD 4). The fact that the two samples underlying dredged spoil piles (GRD 5 and 7) have the lowest pH suggests that groundwater may evolve to higher pH with distance from the acid source (Davis and Runnells, 1987).

Dissolved copper and zinc concentrations are considerably higher in the southern spread area. Concentrations in guard wells GRD 5-8 are three orders of magnitude higher than ambient water quality criteria (USEPA, 2000). Using dissolved sulfur, copper, and zinc concentrations from GRD 4 (and average iron concentrations from MW 20), the relative stability fields of metal aqueous and solid phases were estimated and compared to groundwater compositions (Figure E-1-2 through E-1-4). As shown on the figures, oxidized groundwater is unsaturated with respect to iron, copper, and zinc-bearing minerals with increased acidity. There is also a clear correlation between increasing acidity and dissolved metal concentrations, suggesting reactions such as E-1 through E-4 are operative.

### **Adsorption and Desorption Processes**

Adsorption is, strictly speaking, the process where dissolved metal ions or complexes attach themselves to the surface of particulate matter without forming a three-dimensional molecular structure. Desorption, by contrast, is the detachment of the metal from the surface and its return to the dissolved state. Adsorption and desorption can be empirically expressed in terms of second-order reactions of the form:



where  $M_i$  = the  $i^{\text{th}}$  dissolved metal concentration (or activity);  $S_j$  = the  $j^{\text{th}}$  surface site concentration located on the sediment; and  $M_iS_j$  = the adsorbed metal complex (Luoma 1990). Using this representation, the distribution of a metal between the aqueous and solid phases is governed by the following expression:

$$K_d = M_iS_j / (M_i * S_j) \quad (E-1-7)$$

where  $K_d$  is the distribution coefficient of the metal and is equal to the equilibrium reaction constant for a given temperature and pressure. Equation 3.5-7 implies that if additional dissolved

metal or surface sites are added to the water column (i.e.,  $M_i$  or  $S_j$  increase), then the concentration of adsorbed metal  $M_iS_j$  will increase at the expense of  $M_i$  and  $S_j$  until the equality is restored.

Distribution coefficients between dissolved and adsorbed (i.e. adsorbed and precipitated) metals were calculated from SSB sediment and total aqueous concentrations (note: although total aqueous concentrations are not necessarily representative of dissolved concentrations, they are similar if suspended sediment concentrations are low). For copper, average values for the northern and southern project site are approximately 10,000 L/kg and 27,000 L/kg, respectively (Table E-1-1). These numbers are similar to ambient Bay values of 34,000 L/kg; however, there is high variability between samples. For zinc, values for the northern and southern areas are approximately 6,000 L/kg and 9,000 L/kg, respectively. These are considerably less than Bay values of 350,000 L/kg, indicating a relative preference for the dissolved state.

The general increase in  $K_d$  values from north to south is displayed on Figure E-1-5. Neglecting the possibility that there are systematic differences in total suspended sediment in the samples (TSS should be small if sampling is performed carefully), spatial differences in distribution coefficients represent actual differences in soil and groundwater chemistry.

The inferred effect of soil-controlled processes on distribution coefficients is displayed as dashed curves on Figures E-1-6a through E-1-6c. The dashed curves on the Figure E-1-6a represents trends that would be expected if surface sites in the southern area had reached capacity due to higher metal contamination levels in the groundwater. Similarly, the curves on Figure E-1-6b represent the condition where dissolved concentrations are controlled by adsorption in the north (SSB 1 through 3), but are controlled by precipitation at higher dissolved concentrations measured in the southern spread (SSB 4 through 8). Finally, the circled area on Figure E-1-6c represents data that could be explained by remnant metal sulfides minerals in the southern spread area causing the numerator in equation (E-1-7) to be higher. Clearly, neither of the first two possibilities adequately characterizes the data. Although the third possibility is consistent with all but one datum for copper, it is inconsistent with the trends for zinc.

The effect of varying porewater concentrations on distribution coefficients is shown as the solid and dashed curves on Figures E-1-7a and E-1-7b. The curves match the data reasonably well, which is consistent with the lower water hardness and higher aqueous organic matter measured in the southern guard wells (Table E-1-2). Less calcium and magnesium means there is less competition for surface sites, more adsorption by copper and zinc, and subsequently higher distribution coefficients. Also, higher levels of metal-organic complexation has been shown to produce a ten thousand times increase in adsorption (Davis, 1984). Organic-controlled adsorption would be expected to produce an adsorption maxima in slightly acidic fluids for a fixed amount of organic matter. There may be a peak distribution coefficient on Figure E-1-7c, but there is also significant scatter, and the exact role of organic complexation cannot be determined from the data.

### **Precipitation and Dissolution Processes**

As indicated by reactions (E-1-3) and (E-1-4), dissolution of metal-bearing sulfide phases is predominantly controlled by redox processes. Although the data presented on Figure 3.5-2 through Figure 3.5-5 suggests that reaction products are stable in the aqueous phase, these conclusions are based on a restricted thermodynamic dataset and projections using fixed

concentrations of sulfur, copper, and zinc in the groundwater. Consequently, to resolve the issue of whether stable mineral phases limit groundwater transport of copper and zinc, speciation calculations were performed using the inferred groundwater chemistry of two end-member samples representing anoxic and oxic chemistry (GRD 1 and GRD 5), and the numerical method described in Appendix E-3.

According to the results of this analysis, copper and zinc in GRD 5 are predicted to exist in the aqueous phase as carbonate and organic complexes and as uncomplexed ions (Table E-1-2). Solutions are also predicted to be saturated or supersaturated with respect to gypsum ( $\text{CaSO}_4 \cdot 2\text{H}_2\text{O}$ ), jarosite ( $\text{KFe}_3(\text{SO}_4)_2(\text{OH})_6$ ), lepidocrocite ( $\text{FeOOH}$ ), and cupric ferrite ( $\text{CuFe}_2\text{O}_4$ ). Finally, equilibration of GRD 5 with these mineral phases leads to cupric ferrite and gypsum precipitation and a decrease in dissolved copper concentrations by approximately 0.150 mg/L (a large drop relative to WQO, but only a fraction of the total dissolved copper concentration).

Analogous modeling of the less acidic GRD 1 well shows that copper and zinc are almost entirely complexed with organic ligands. Although this solution is supersaturated with respect to calcite ( $\text{CaCO}_3$ ), jarosite ( $\text{KFe}_3(\text{SO}_4)_2(\text{OH})_6$ ), ferrihydrite ( $\text{Fe}(\text{OH})_3$ ), lepidocrocite ( $\text{FeOOH}$ ), and cupric ferrite ( $\text{CuFe}_2\text{O}_4$ ), equilibration only results in precipitation of lepidocrocite and calcite.

### **Discussion**

Elevated concentrations of copper and zinc are generated in the shallow groundwater by the oxidation of metal-bearing sulfide minerals. Once in solution, the primary factor controlling retardation of copper and zinc is predicted to be metal sorption. To demonstrate this conclusion, GRD 5 and GRD 1 well waters were equilibrated with inferred surfaces at the site using a method described in Appendix E-3. As shown in Table E-1-2, dissolved concentrations are approximately  $\frac{1}{2}$  the initial values for GRD 5, but are identical for GRD 1. Greater adsorption in GRD 5 is consistent with higher metal concentrations in solution and the relationship expressed in equation (E-1-7). It is also consistent with the larger equilibrium distribution coefficients measured in the southern spread area (Figure E-1-5).

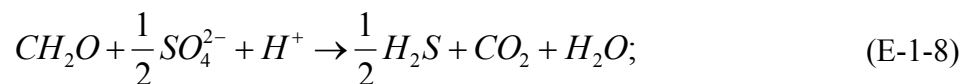
Dissolved copper and zinc are unlikely to be affected by precipitation of oxidized mineral phases. Although some copper attenuation may be provided by cupric ferrite (GRD 5), this phase is relatively soluble, and will dissolve as groundwater concentrations of iron and copper diminish (GRD 1).

## **E-1.3 Deep Groundwater Transport**

### **Introduction**

The second zone where metal transport occurs is defined by the active microbiological reduction of organic matter by anaerobic bacteria. This zone is typically found within tens of centimeters below the water table (Parkes et al., 1993), but may be deeper at the project site. The primary process affecting acidity and dissolved metal concentrations in this zone is the progressive drop in the oxidation state of the system with depth. This anoxia is created by the sequential oxidation of organic carbon through denitrification, nitrate reduction, Mn(II) solubilization, fermentation, Fe(II) solubilization, sulfate reduction, and finally, methane formation (Stumm and Morgan,

1996). All but one of these reactions consume solution acidity. Also, the sulfate reduction reaction:



enhances metal precipitation through:



Despite the fact that acid is generated during precipitation, the amount produced is less than that consumed by the reduction process because metals are generally present in trace quantities (Garcia et al. 2001).

### **Summary of Field Data**

Laboratory chemical characterization of deep groundwater was undertaken in this study to predict project-induced changes in contaminant mobility in anoxic environments. Deep groundwater has been monitored since 1987, and the results of the most recent monitoring activities (11/02) and long-term averages since 1993 (when lower detection limits were implemented) are displayed in Table E-1-3 for twelve MW wells underlying dredged spoil piles. These wells were screened at minimum depths of 4.5 to 15 feet below the ground surface.

According to the results of the measurements, there is greater variability in pH and dissolved metal concentrations in the southern spread area. There is also detectable quantities of dissolved sulfide in most samples. This is evident on Figure E-1-1, where the oxidation state and pH of the samples are plotted as solid circles (using equation (E-1-5) and sulfate/sulfide concentrations instead of aqueous and gaseous oxygen). Samples north of the tide gate cluster near neutral pH in the stability field of sulfide. Samples MW 19 and MW 25 are more acidic and lie approximately at the sulfate/solid sulfur boundary.

Dissolved copper and zinc concentrations are lower in deep groundwater compared to shallow, and median concentrations for copper are equal to the detection limit (Table E-1-3). For zinc, average and median concentrations are only above ambient Bay water quality criteria for MW 3A, MW 19, and MW 25 (two of the three shallowest wells). According to the results in Figures E-1-2 through E-1-4, deep groundwater appears to be saturated or supersaturated with respect to pyrite ( $FeS_2$ ), covellite ( $CuS$ ), and sphalerite ( $ZnS$ ). This implies that many of the measured groundwater samples are in a state of disequilibrium.

### **Adsorption and Desorption Processes**

Because distribution coefficients were not measured in this study, the importance of adsorption processes on two end-member groundwater solutions (MW-25 and MW-20) was estimated using the mass action/mass balance approach described in Appendix E-3. After equilibrating sorbing surfaces with copper and zinc-free groundwater, surfaces were re-equilibrated with metal-bearing solutions.

The results of these numerical sorption experiments are shown in Table E-1-4. Whereas zinc concentrations are predicted to drop 8 mg/L in MW 25, copper is relatively unchanged. This latter observation is a consequence of the fact that copper is predicted to be in a +1 oxidation state and cannot adequately compete for surface sites with calcium, zinc, and other +2 ions. At lower dissolved concentrations of zinc and copper (i.e. MW 20), sorption does not appreciably reduce groundwater concentrations of copper and zinc.

### **Precipitation and Dissolution Processes**

In contrast to oxidized fluids, dissolved copper and zinc concentrations under reducing conditions may be buffered by sulfide mineral phases at equilibrium. According to the results of Table 1 for MW 25, copper is predicted to exist as chloride and sulfide complexes and zinc is predicted to exist as uncomplexed ions (Table E-1-4). Equilibration with supersaturated mineral phases results in precipitation of covellite (CuS).

For MW 20, copper and zinc are both predicted to exist as sulfide complexes in the aqueous phase. Equilibration of this more reduced fluid results in the precipitation of chalcocite (Cu<sub>2</sub>S) and sphalerite (ZnS). Also, dissolved concentrations of copper and zinc are 0.003 and 0.002 mg/L, respectively.

### **Discussion**

Model predictions show that zinc has a high capacity to sorb at dissolved concentrations greater than 1 mg/L. Copper, by contrast, is in a +1 oxidation state and does not effectively compete for surface sites. In opposition to shallow groundwater, the primary attenuation mechanism below the zone of sulfate reduction is precipitation of copper and zinc sulfide phases. Dissolved copper and zinc concentrations in equilibrium with metal sulfide phases are predicted to be at or below current detection limits.

The reason that measured groundwater concentrations are higher in some wells than would be expected if solutions were buffered by metal sulfides is that the equilibration process is slow. For example, inorganic reduction of sulfate to sulfide is on the order of 2 mg/L/yr at a pH of 2.0, but  $9 \times 10^{-17}$  mg/L/yr at a neutral pH (Table E-1-5). Consequently, the only reason that sulfide is produced at all in nature is that the actual reduction process occurs via reaction (E-1-8), which is microbiologically catalyzed. For marine and estuarine systems, this reaction rate is on the order of  $10^3$  mg/L/yr. Although lower rates have been observed in sandy aquifers, it has also been found that these are caused by low concentrations of organic carbon. The amount of organic carbon in the study of Jakobsen and Postma (1999) was approximately 0.01%, whereas the concentrations in this study are more greater by a factor of 100.

Because metal reduction and precipitation rates have been found to be on the order of days (Table E-1-5), it might be expected that sulfate reduction is the rate-limiting step of the precipitation process; however, this is inconsistent with the relatively high dissolved copper and zinc concentrations in the sulfide-bearing waters of the project site. Because the exact mechanism limiting precipitation is unidentified, site-specific rates of sulfate reduction and metal precipitation were estimated from long-term groundwater monitoring data. On Figure E-1-8, copper concentrations in twelve MW wells are shown to generally be below detection limits until the period 1996-1998, when the Bay Area experienced two above average precipitation years (1996 and 1998) and a large precipitation event (the “Great Flood” of 1997). Not only do the

earliest and largest spikes in copper and zinc concentrations occur in the shallowest wells (MW-3A and MW-25), but concentrations gradually return to detection limit values with time in most wells. Consequently, dissolved copper and zinc concentrations likely fluctuate with time due to surface recharge of oxidized, acidic fluids during periods of high precipitation. Without additional surface recharge, copper and zinc concentrations drop below detection limits after 0-2 years, presumably through a precipitation mechanism.

#### **E-1.4 Conclusions**

The primary attenuation mechanism in shallow, oxidized groundwater is adsorption onto organic matter in the root zone. Although precipitation of copper may occur near the acid source, its solubility is high, and will dissolve in more dilute aqueous solutions. Distribution coefficients measured in shallow groundwater show a spatial dependence, with higher adsorbed fractions in the southern spread area. This may be caused by remnant sulfides biasing measurements, or it may be real, and due to less water hardness and more aqueous organic matter in the southern guard wells. Additional sampling is required to resolve this issue.

Attenuation in the zone of active sulfate reduction (deep groundwater) is not driven by surface complexation reactions. Although a fraction of zinc may be sorbed at high concentrations, this attenuation mechanism becomes less effective at lower dissolved concentrations. Also, copper does not effectively compete for surface sorption sites because it is in a +1 oxidation state. Attenuation in deeper groundwater is instead controlled by precipitation of insoluble copper and zinc sulfides. Solutions in equilibrium with these solid phases are predicted to have concentrations below current detection limits. Laboratory and field evidence suggest that this precipitation process may take between 0 and 2 years.

Future removal of dredged spoil piles should cause concentrations in deep groundwater to fall below current detection limits because metal sulfides will be removed from the zone of active oxidation. By contrast, the rate and magnitude of decline in shallow groundwater is difficult to quantify. In the short-term, concentrations will be controlled by equilibrium distribution coefficients between aqueous and sorbed metal species; however, if pH recovers to more neutral conditions near the area where spoil piles now exist, bacterial sulfate reduction may occur at shallower depths (Garcia et al., 2001). This process may already be occurring in areas distal to the spoils, but cannot be verified due to biased shallow groundwater sampling (i.e. SSB wells were sampled below existing spoil piles and the GRD wells were contaminated by near-surface water).

Based on these conclusions, average distribution coefficients were calculated from the data in Table E-1-5 to estimate concentrations of copper and zinc in groundwater seepage into the realignment. These values were subsequently used in the MIKE 21 ME sediment and water quality model to assess the potential for recontamination of the realignment (Section 3.5.6). Because most copper and zinc sulfides will be removed from areas of active oxidation, groundwater will likely be less contaminated than current conditions. Consequently, model results are conservative.

**Appendix E-2**  
**Results of MIKE Surface Water Quality Model**

Figure E2 – 1 Bathymetry Used in the MIKE21 Model for Erosion Calculations (With spoil piles)

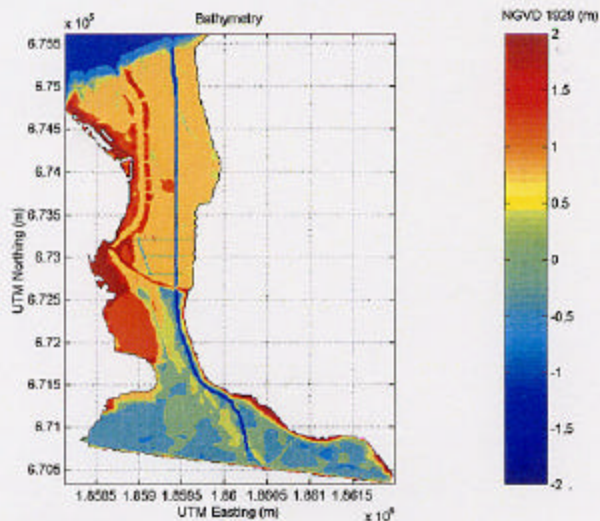


Figure E2-2 Mean Shear From MIKE21 Model Results for Erosion Calculations (With spoil piles)

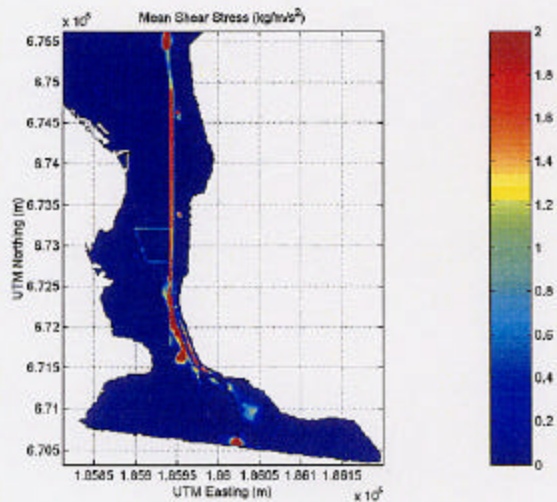


Figure E2 – 3 Shear Stresses that Exceeded a Critical Shear Stress of  $0.40 \text{ N/m}^2$  (typical for weakly consolidated sediment) from the MIKE21 Model Results for Erosion Calculations (With spoil piles)

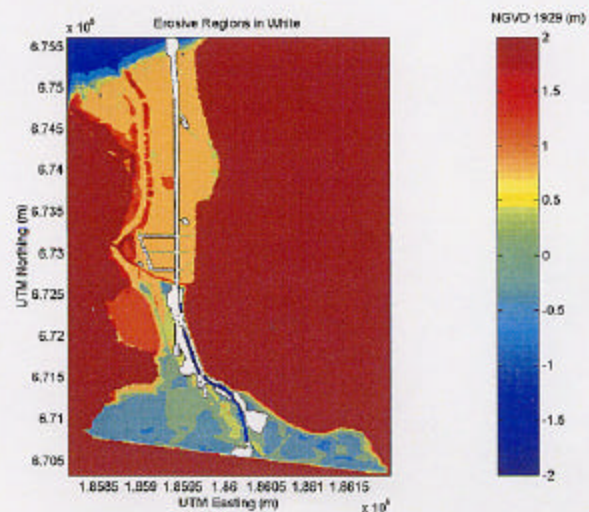


Figure E2 – 4 Bathymetry Used in the MIKE21 Model for Erosion Calculations Without spoil piles

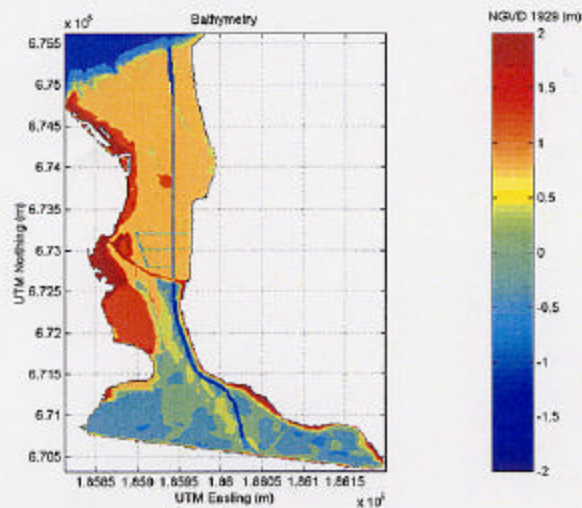


Figure E2-5 Mean Shear From MIKE21 Model Results for Erosion Calculations (Without spoil piles)

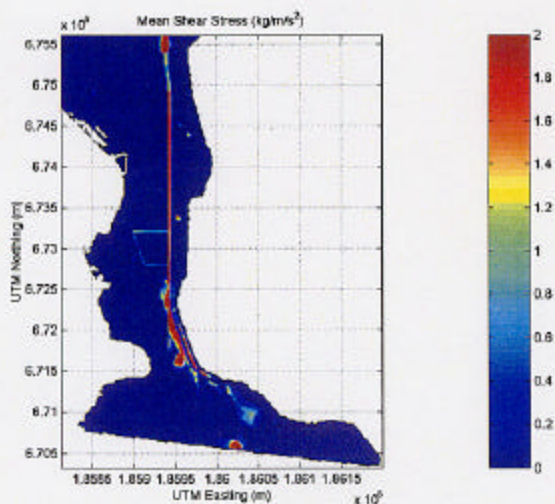
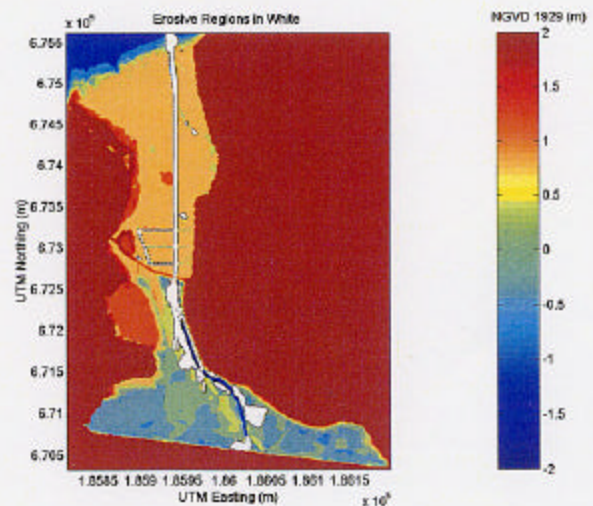
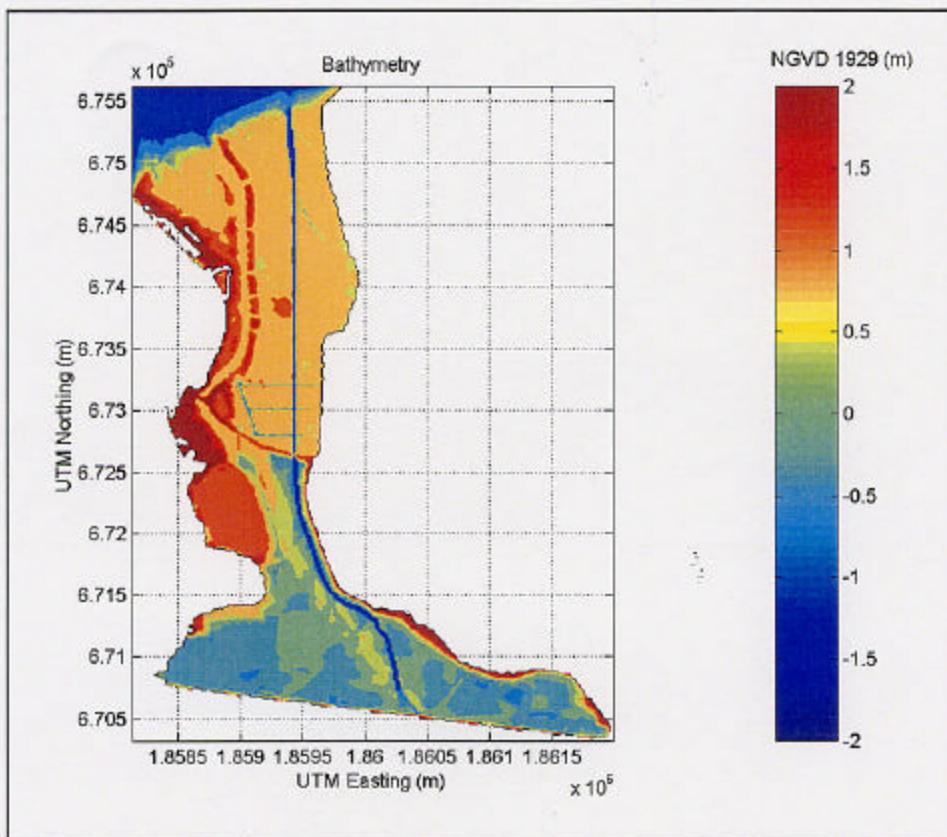
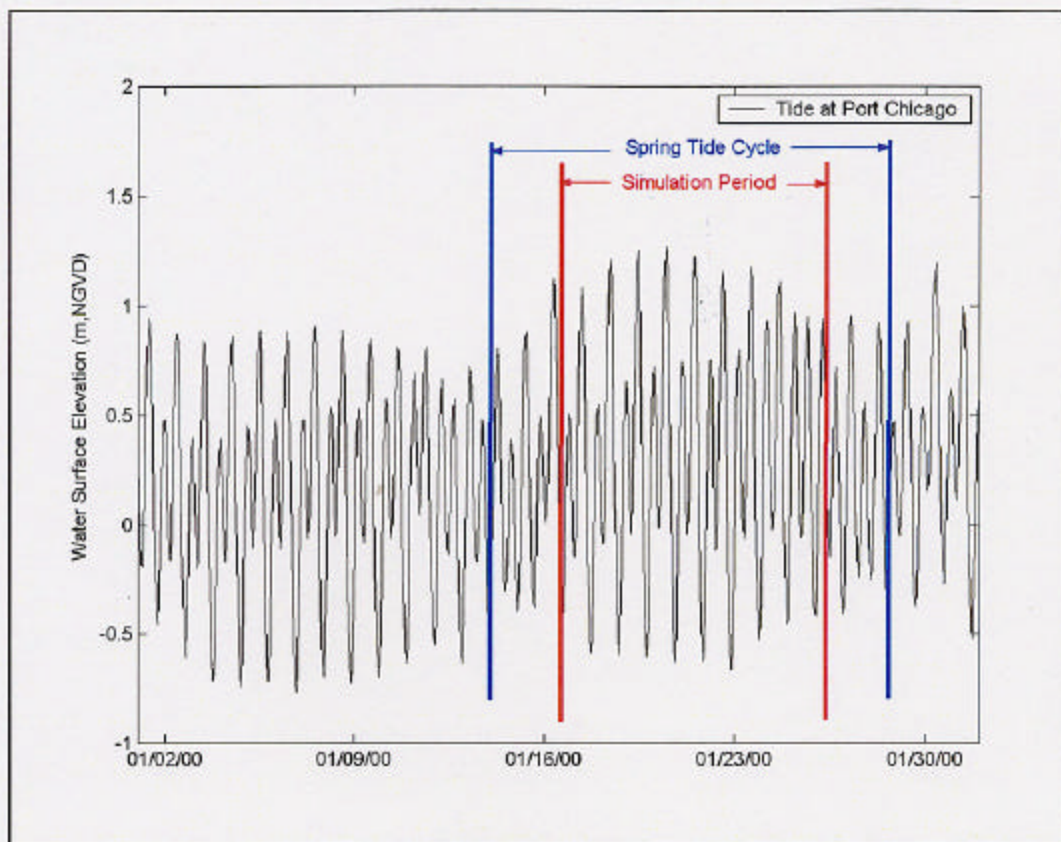


Figure E2 – 6 Shear Stresses that Exceed a Critical Shear Stress of  $0.40 \text{ N/m}^2$  (typical for weakly consolidated sediment) from the MIKE21 Model Results for Erosion Calculations (Without spoil piles)

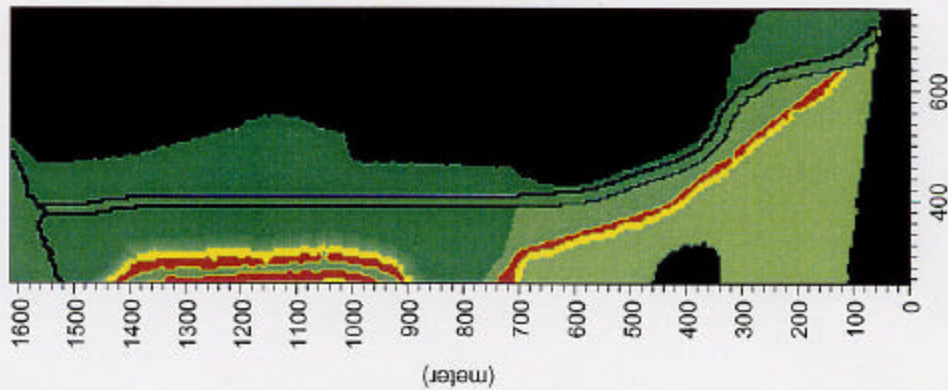




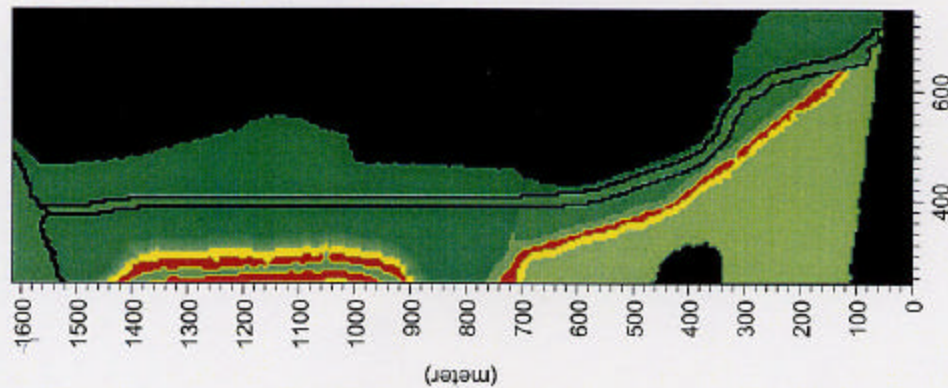
**Bathymetric surface modeling domain. Elevations indicated are meters in NGVD 1929.**



Tide Used in MIKE21 Water Quality and Erosion Analysis



CASE 1: FILL TO ERM



CASE 2: FILL TO BACKGROUND

Cu Total (mg/kg)

Above 900
800 - 900
700 - 800
600 - 700
500 - 600
400 - 500
300 - 400
200 - 300
150 - 200
100 - 150
50 - 100
10 - 50
Below 10

**URS**

Client:

RHODIA MARTINEZ

Project:

REMEDIAL DESIGN REPORT PEYTON SLOUGH

Date: 03/02

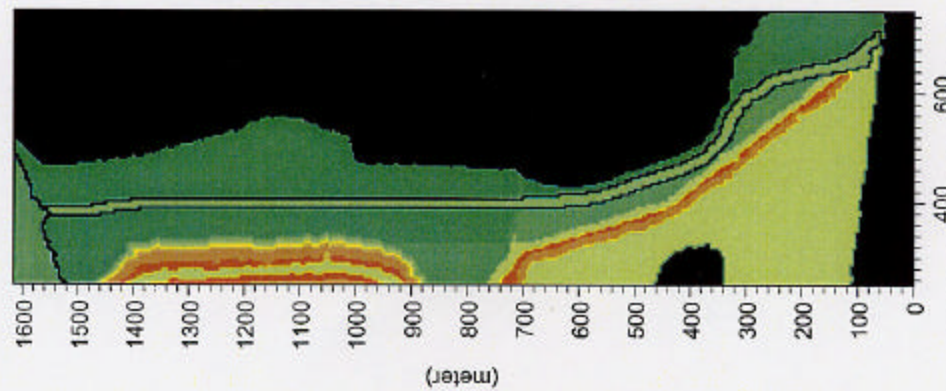
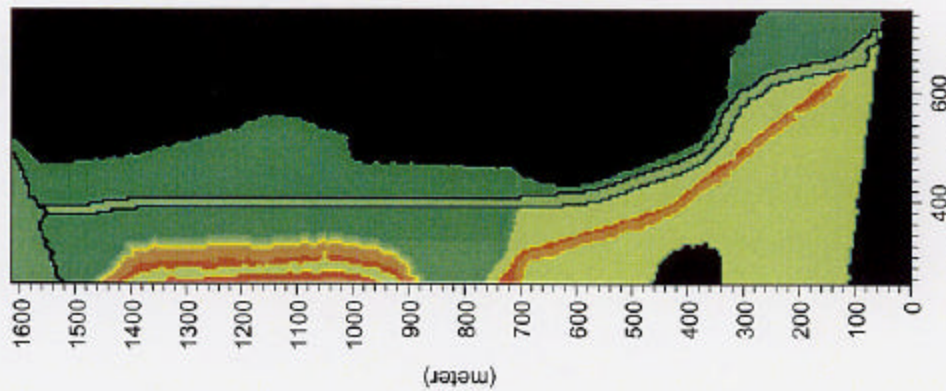
Init: BB

SEDIMENT COPPER CONCENTRATIONS (mg/kg)  
USED IN MIKE 21 ME MODEL--ONLY PARTIAL  
AREA SHOWN (REALIGNMENT OUTLINED)

Drawing no.

FIG. E2-7

MIKE21



Zn Total (mg/kg)

Above 900  
800 - 900  
700 - 800  
600 - 700  
500 - 600  
400 - 500  
300 - 400  
200 - 300  
150 - 200  
100 - 150  
50 - 100  
10 - 50  
Below 10

D:\RhodiaData\env\mex\Results\Zn\_1.dkt2

D:\RhodiaData\env\mex\Results\Zn\_4.dkt2

**URS**

Client:

RHODIA MARTINEZ

Project:

REMEDIAL DESIGN REPORT PEYTON SLOUGH

SEDIMENT ZINC CONCENTRATIONS (mg/kg)  
USED IN MIKE 21 ME MODEL—ONLY PARTIAL  
AREA SHOWN (REALIGNMENT OUTLINED)

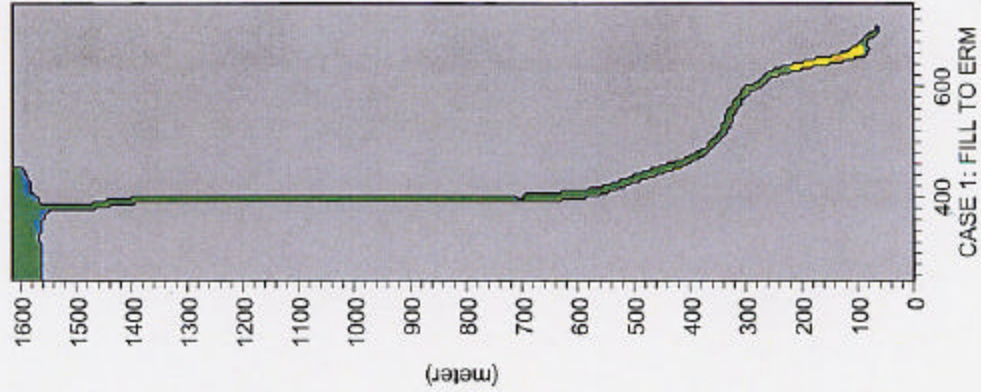
Date: 03/02

Init: BB

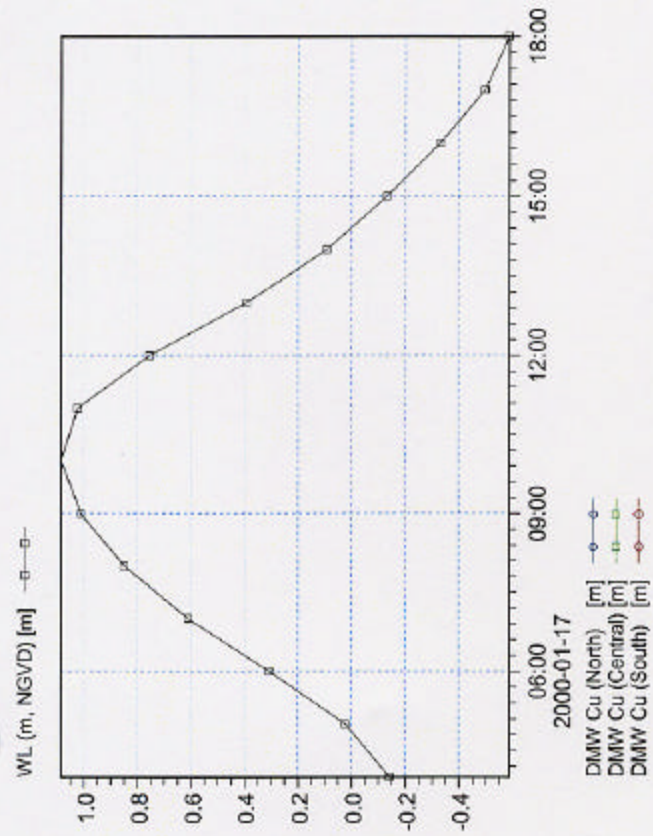
Drawing no.

FIG. E2-8

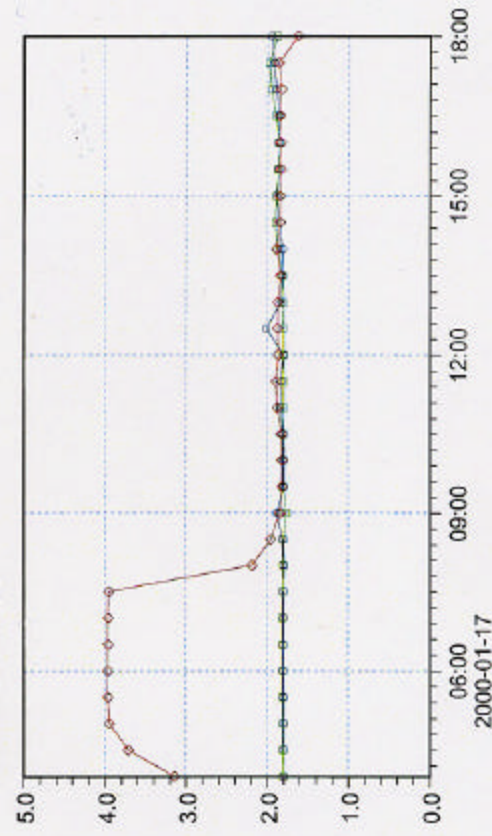
MIKE21



D:\RhodiaData\hydro\me\FlowRateR\_FlowRateR\_DMW\_R1.d12



D:\RhodiaData\hydro\me\FlowRateR\_FlowRateR\_DMW\_R1.d12

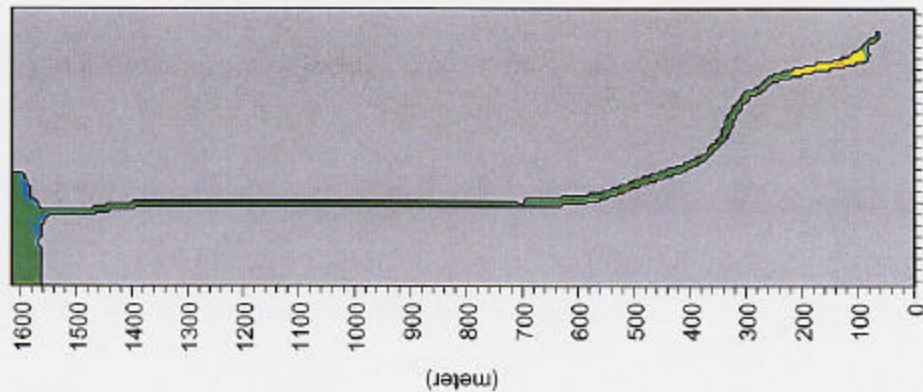


D:\RhodiaData\hydro\me\FlowRateR\_FlowRateR\_DMW\_R1.d12

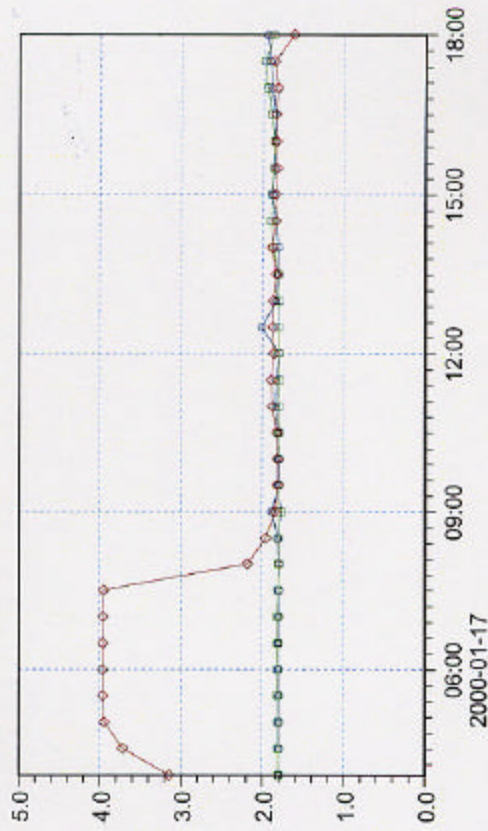
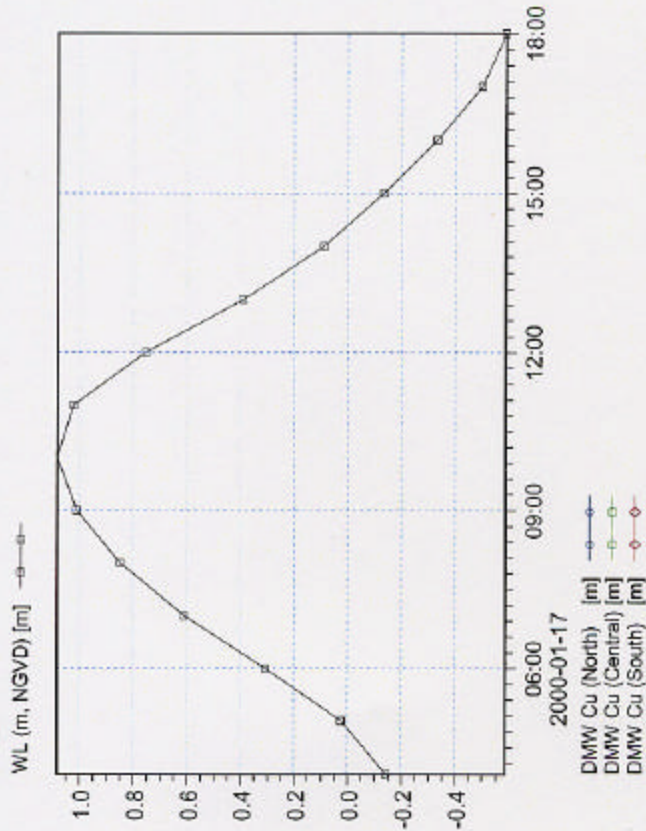
Client: RHODIA MARTINEZ		Project: REMEDIAL DESIGN REPORT PEYTON SLOUGH	
Date: 03/02		Drawing no. FIG. E2-9a	
Init: BB		CASE 1 AVERAGE DISSOLVED COPPER (ug/L) IN THE REALIGNMENT (LEFT), WATER LEVEL (m) AND TIME SERIES OF COPPER (ug/L) (RIGHT)	



MIKE2.0



CASE 2: FILL TO BACKGROUND



Client: RHODIA MARTINEZ

Project: REMEDIAL DESIGN REPORT PEYTON SLOUGH

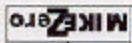
CASE 2 AVERAGE DISSOLVED COPPER (ug/L)  
 IN THE REALIGNMENT (LEFT), WATER LEVEL (m)  
 AND TIME SERIES OF COPPER (ug/L) (RIGHT)

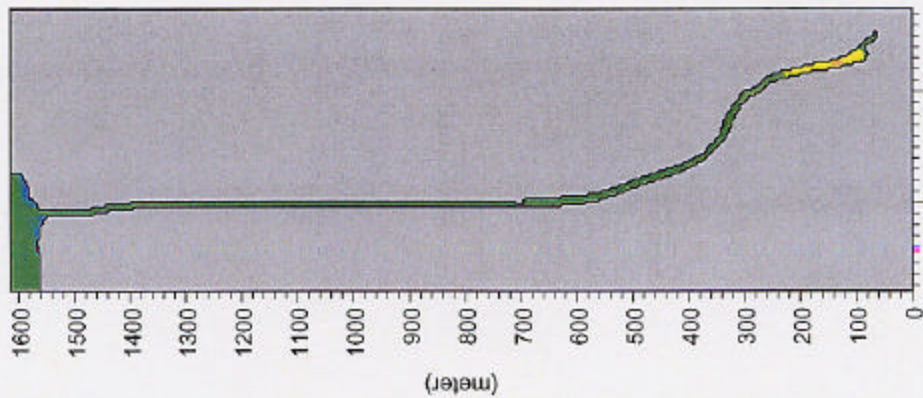
Date: 03/02

Init: BB

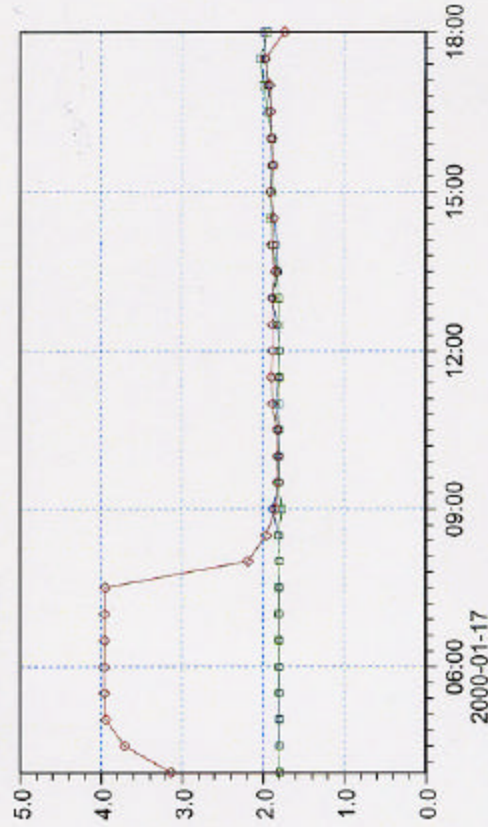
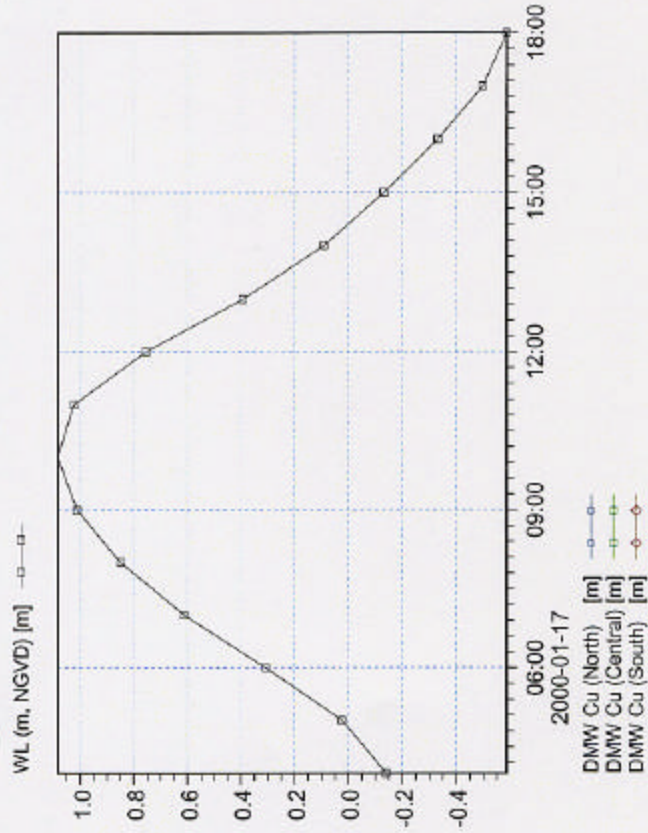
Drawing no.

FIG. E2-9b





CASE 3: 2 x RESUSPENSION



Client:

RHODIA MARTINEZ

Project:

REMEDIAL DESIGN REPORT PEYTON SLOUGH

Date:

03/02

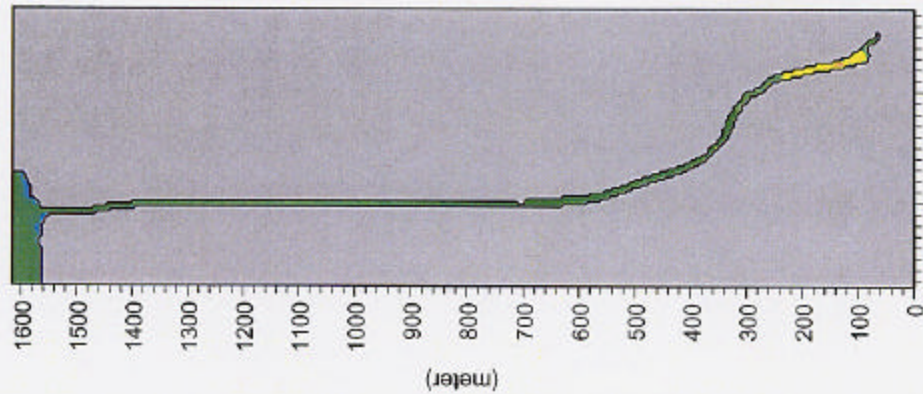
Init:

BB

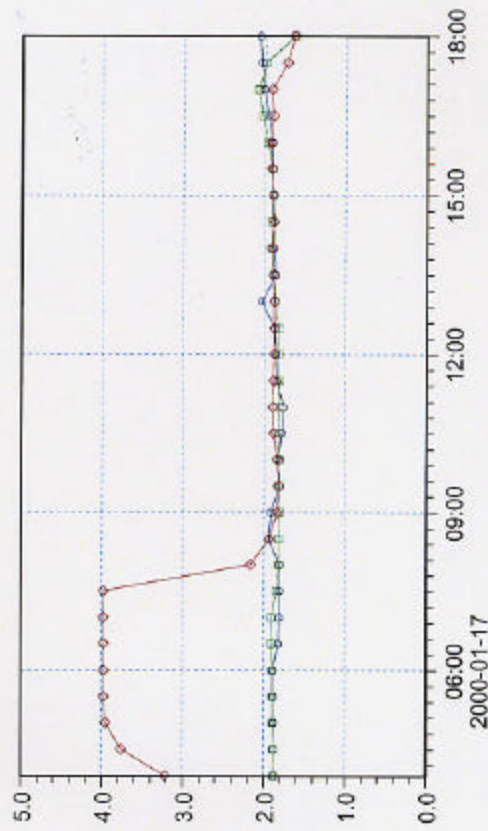
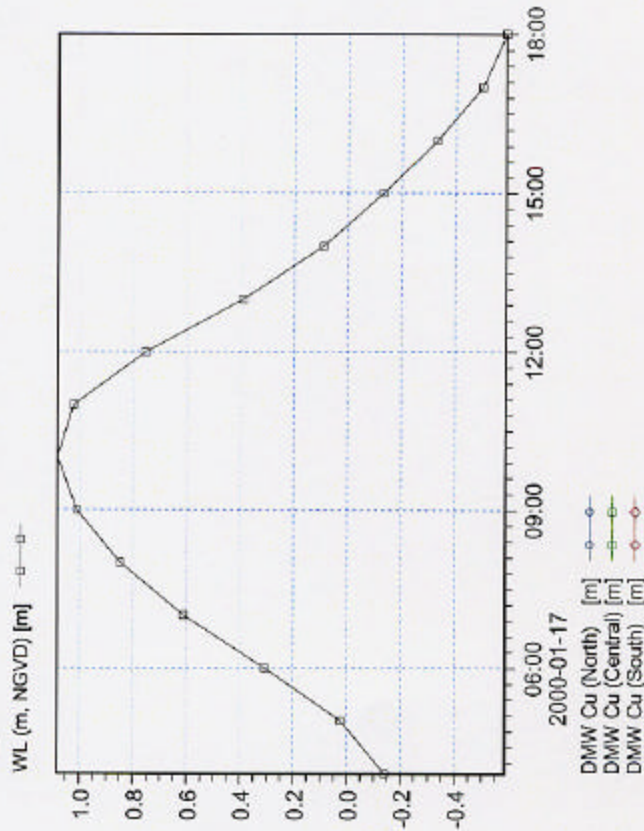
Drawing no.

FIG. E2-9c

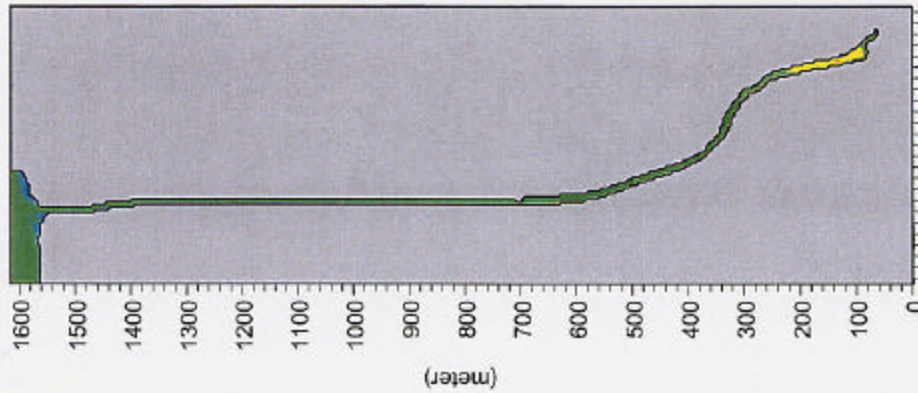
MIKE2.0



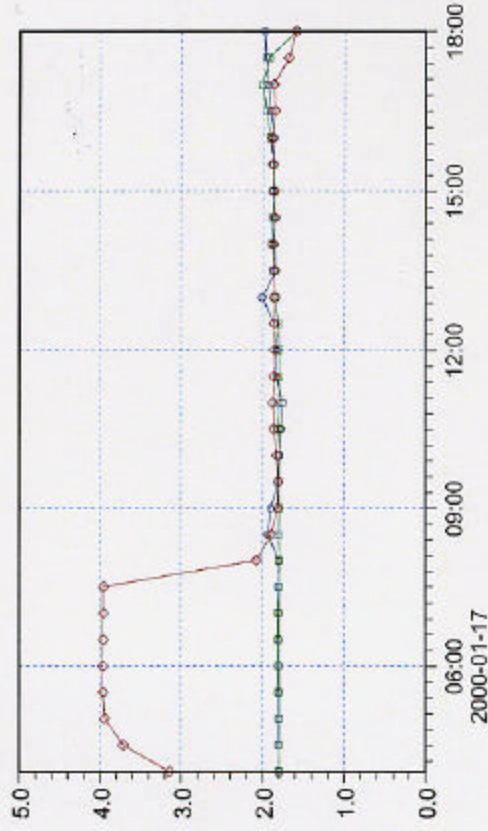
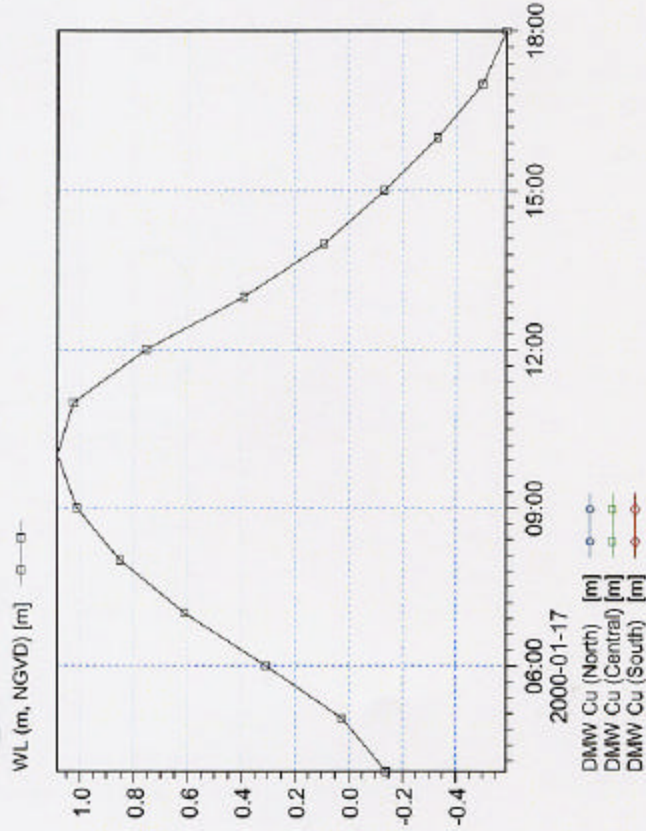
CASE 4: MINIMUM ADSORPTION RATE




<div> <div>URS</div> <div>Client: RHODIA MARTINEZ</div> </div>		<div> <div>MIKE2.0</div> <div>Project: REMEDIAL DESIGN REPORT PEYTON SLOUGH</div> </div>	
Date: 03/02	Init: BB	<div> <div>CASE 4 AVERAGE DISSOLVED COPPER (ug/L) IN THE REALIGNMENT (LEFT), WATER LEVEL (m) AND TIME SERIES OF COPPER (ug/L) (RIGHT)</div> <div>Drawing no. FIG. E2-9d</div> </div>	



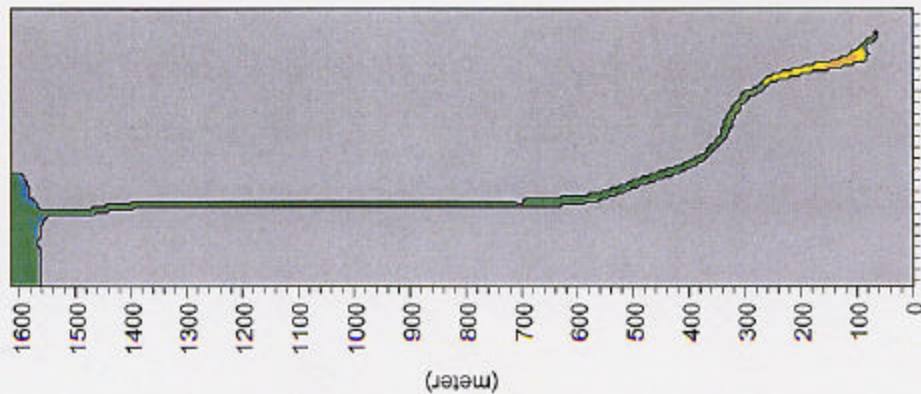
CASE 5: MAX Cu IN REALIGNMENT SEDIMENT



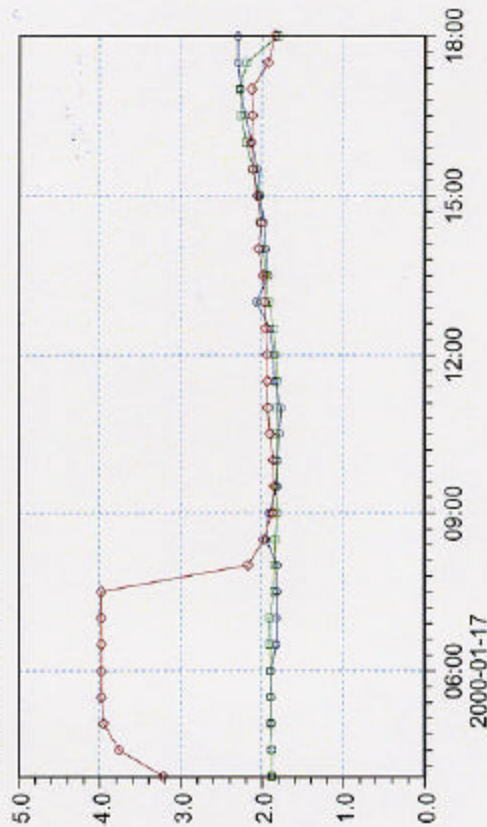
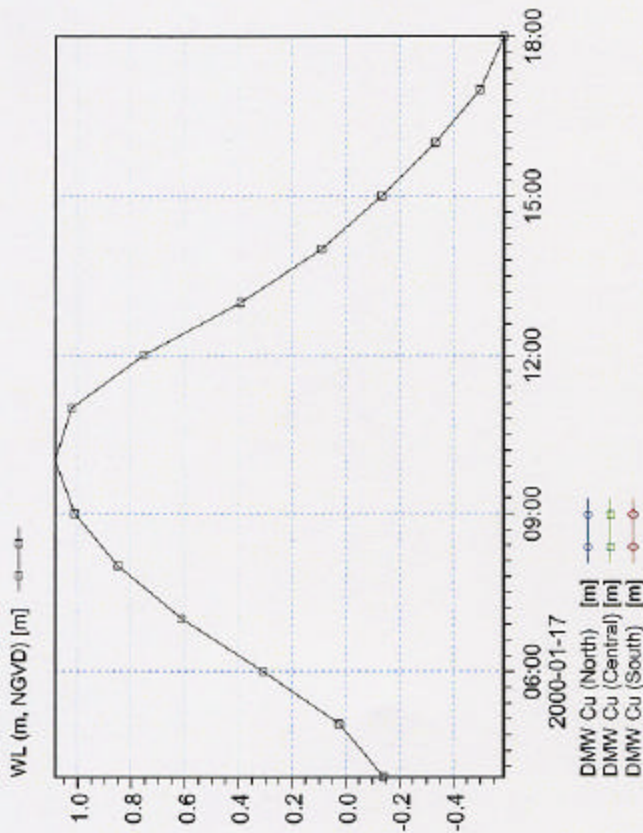
		Client:	RHODIA MARTINEZ	
		Project:	REMEDIATION DESIGN REPORT PEYTON SLOUGH	
Date:	03/02	Drawing no.		FIG. E2-9e
Init:	BB	CASE 5 AVERAGE DISSOLVED COPPER (ug/L) IN THE REALIGNMENT (LEFT), WATER LEVEL (m) AND TIME SERIES OF COPPER (ug/L) (RIGHT)		


D:\Rhodia\Design\Remediation\Results\FINAL FIGURES\PORT\_Chicago.dwg

D:\Rhodia\Design\Remediation\Results\FINAL FIGURES\PORT\_Chicago.dwg



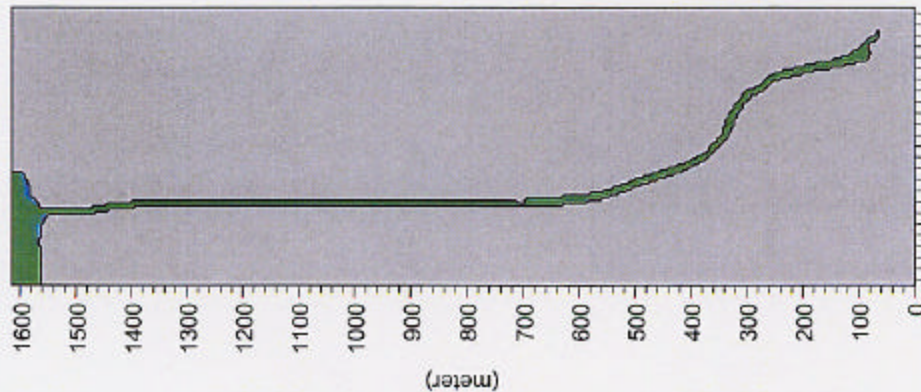
CASE 6: MAX RESUSP. AND Cu AND MIN ADS.



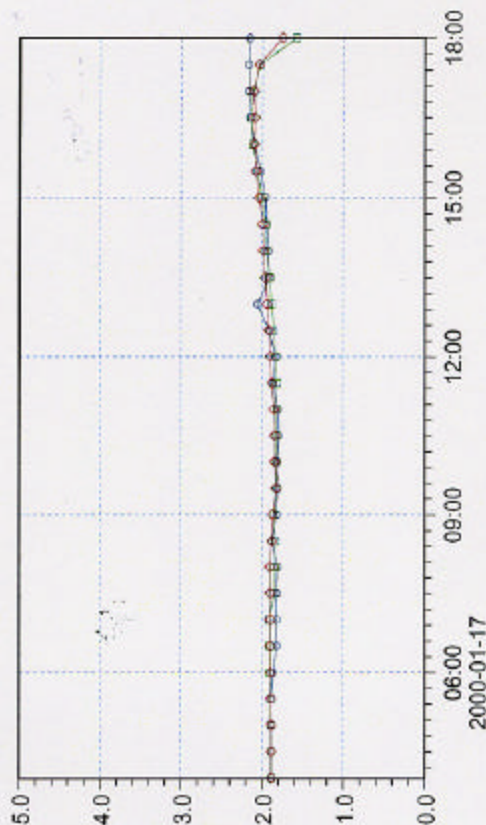
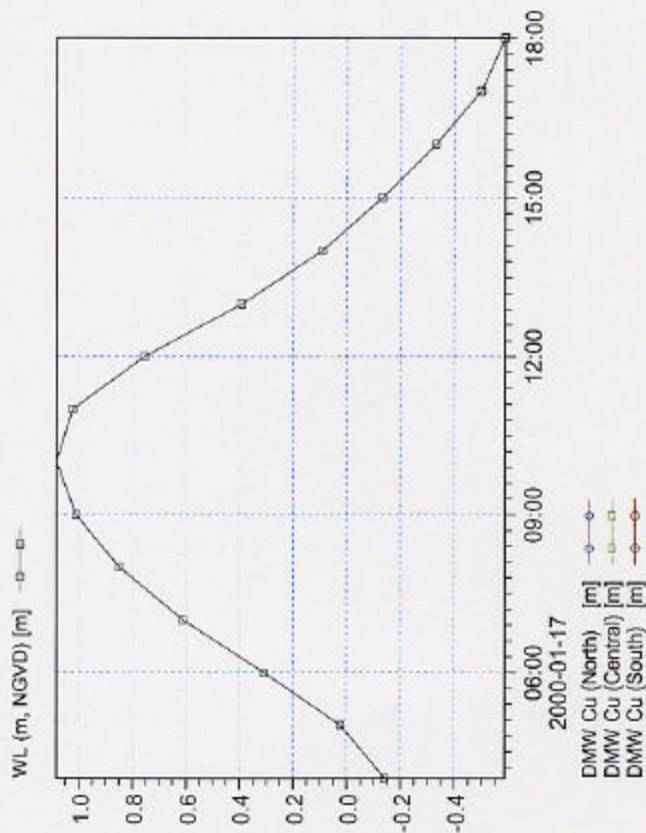
		Client:	RHODIA MARTINEZ	
		Project:	REMEDIAL DESIGN REPORT PEYTON SLOUGH	
Date:	03/02	CASE 6 AVERAGE DISSOLVED COPPER (ug/L) IN THE REALIGNMENT (LEFT), WATER LEVEL (m) AND TIME SERIES OF COPPER (ug/L) (RIGHT)		Drawing no.
Init:	BB			FIG. E2-9f

D:\RhodiaData\Newyork\Rhodia\Final\_FIGURES\Port\_Chicago.dwg


D:\RhodiaData\Newyork\Rhodia\Final\_FIGURES\Port\_Chicago.dwg

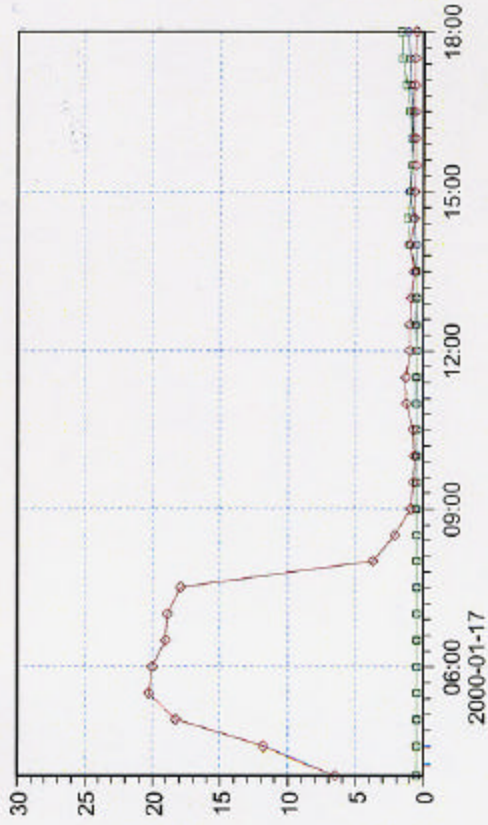
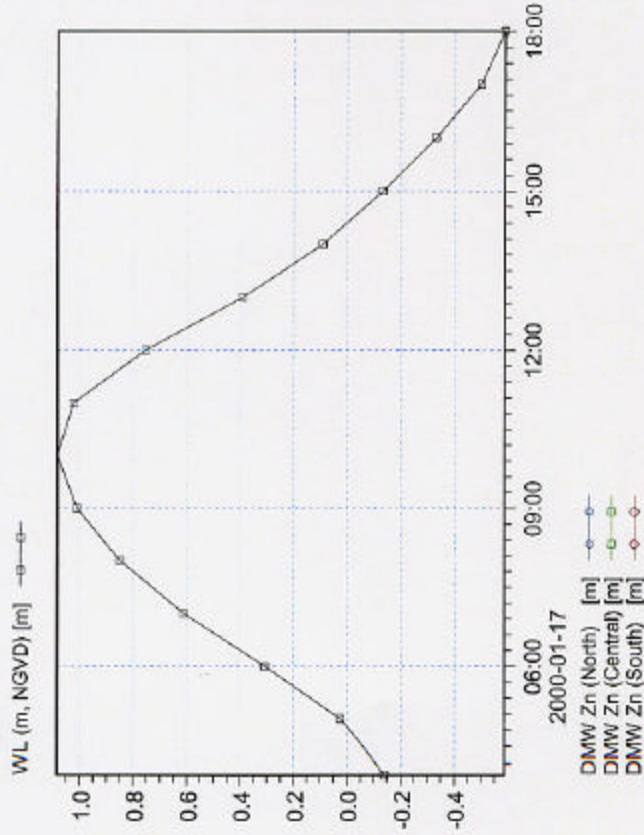
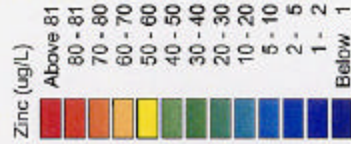
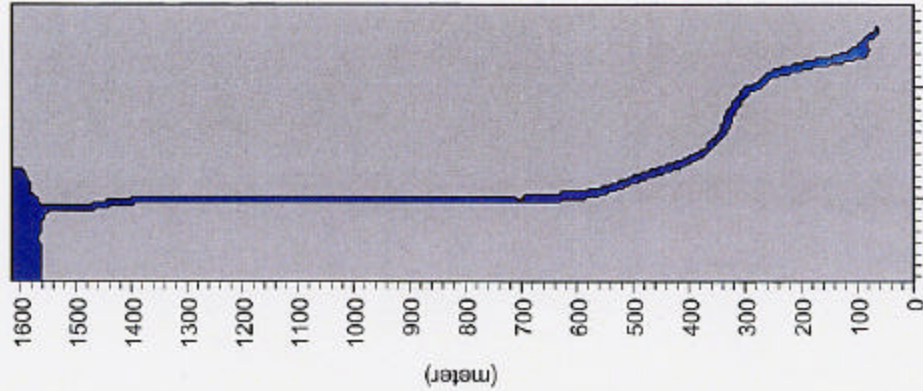


CASE 6 WITHOUT MWSD DISCHARGE



D:\Rhodia\Design\mwsd\results\FINAL FIGURES\_VR\_Plot7.dwg  
 D:\Rhodia\Design\mwsd\results\FINAL FIGURES\_VR\_Plot7.dwg

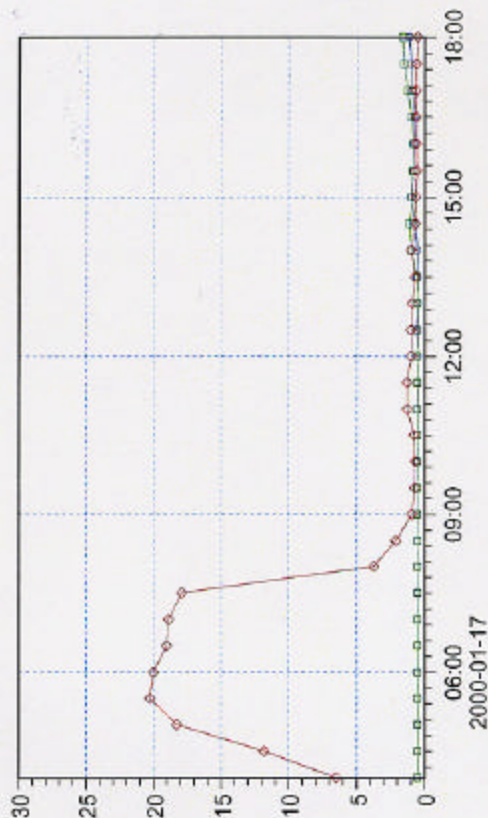
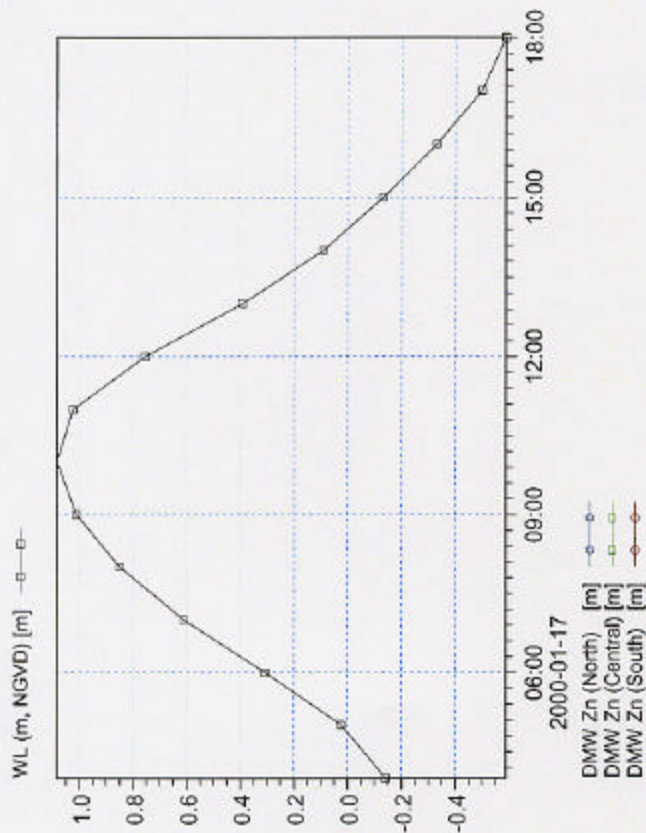
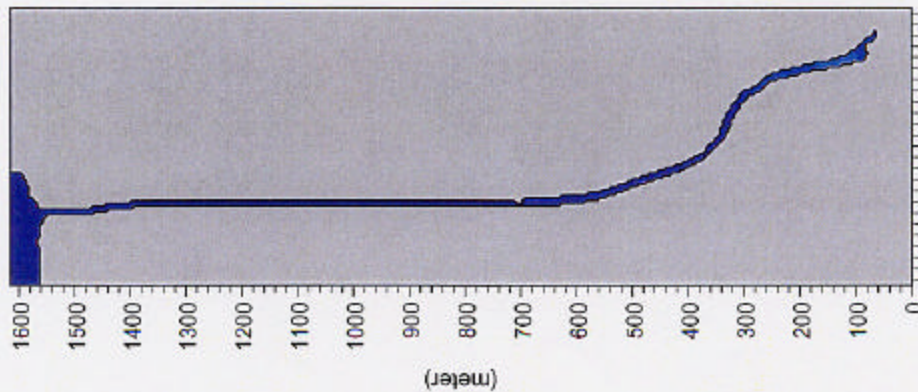
		Client:	RHODIA MARTINEZ	
		Project:	REMEDIATION DESIGN REPORT PEYTON SLOUGH	
Date:	03/02	CASE 7 AVERAGE DISSOLVED COPPER (ug/L) IN THE REALIGNMENT (LEFT), WATER LEVEL (m) AND TIME SERIES OF COPPER (ug/L) (RIGHT)		Drawing no. FIG. E2-9g
Init:	BB			



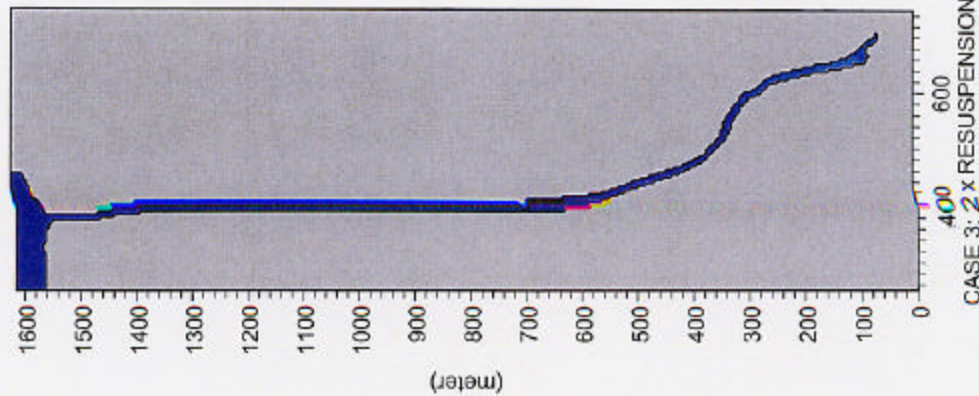
	Client: <b>RHODIA MARTINEZ</b>	<b>REMEDIAL DESIGN REPORT PEYTON SLOUGH</b>	
	Project:	CASE 1 AVERAGE DISSOLVED ZINC (ug/L) IN THE REALIGNMENT (LEFT), WATER LEVEL (m) AND TIME SERIES OF ZINC (ug/L) (RIGHT)	Drawing no. <b>FIG. E2-10a</b>
Date: 03/02	Init: BB		

D:\RhodiaData\history\metals\Final\_Figures\Fig1\_Chicago.d0

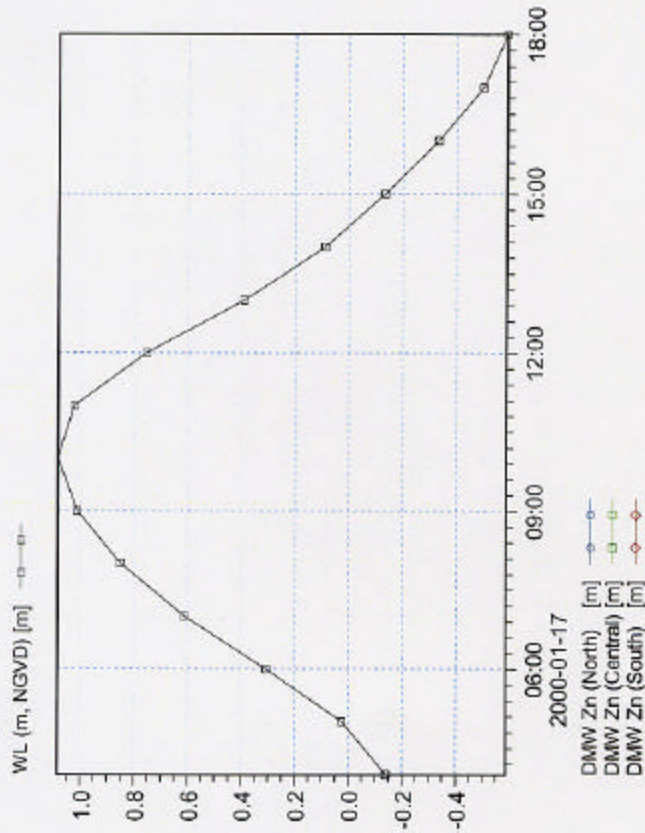
D:\RhodiaData\history\metals\Final\_Figures\Fig1\_Fish\_1.d0



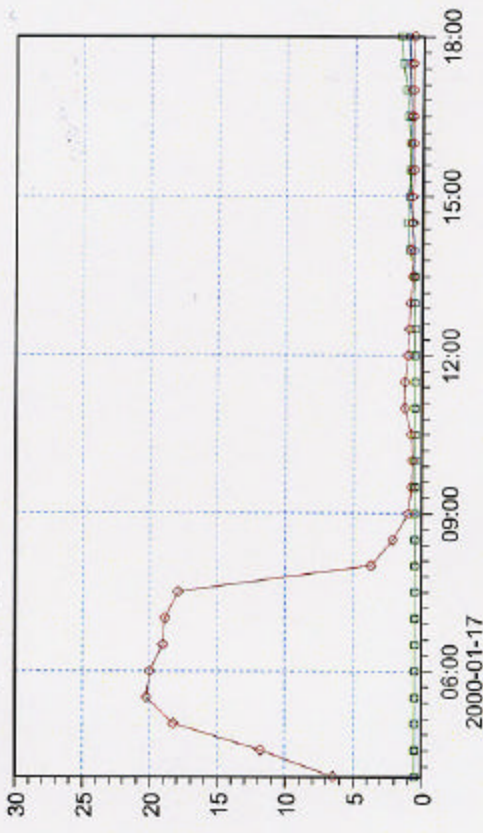
		Client:	RHODIA MARTINEZ	
		Project:	REMEDIATION DESIGN REPORT PEYTON SLOUGH	
Date:	03/02	CASE 2 AVERAGE DISSOLVED ZINC (ug/L) IN THE REALIGNMENT (LEFT), WATER LEVEL (m) AND TIME SERIES OF ZINC (ug/L) (RIGHT)		Drawing no.
Init:	BB			FIG. E2-10b



D:\RhodiaData\new\mex\mex\mex\Figure3\_02



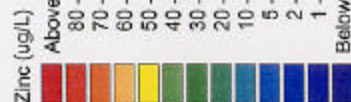
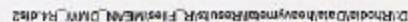
D:\RhodiaData\new\mex\mex\mex\Figure3\_02



D:\RhodiaData\new\mex\mex\mex\Figure3\_02

	Client:	RHODIA MARTINEZ	
	Project:	REMEDIAL DESIGN REPORT PEYTON SLOUGH	
Date:	03/02	CASE 3 AVERAGE DISSOLVED ZINC (ug/L) IN THE REALIGNMENT (LEFT), WATER LEVEL (m) AND TIME SERIES OF ZINC (ug/L) (RIGHT)	
Init:	BB		
		Drawing no.	FIG. E2-10c

MIKEZero



2000-01-17

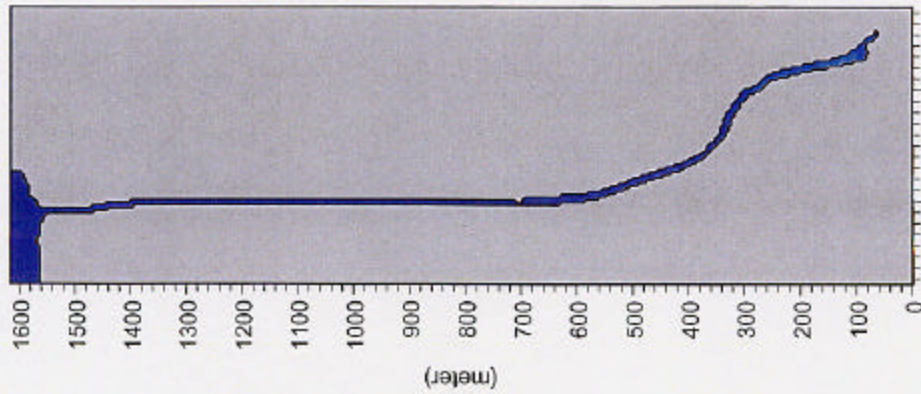
RHODIA MARTINEZ

REMEDIAL DESIGN REPORT PEYTON SLOUGH

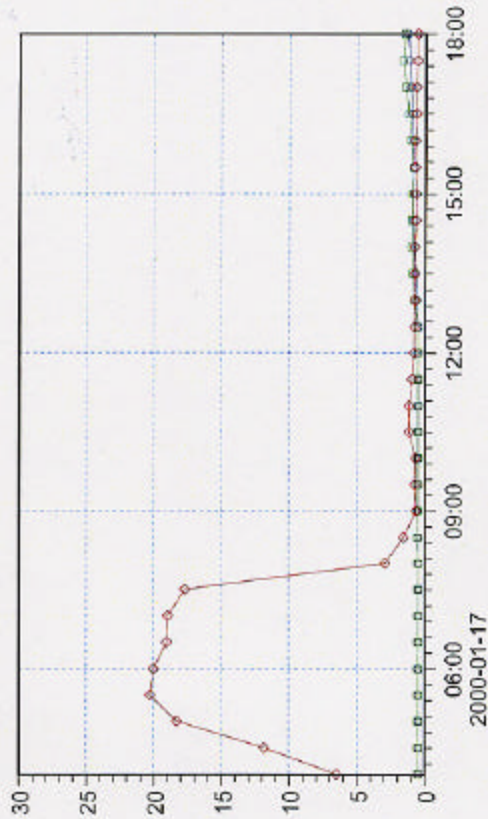
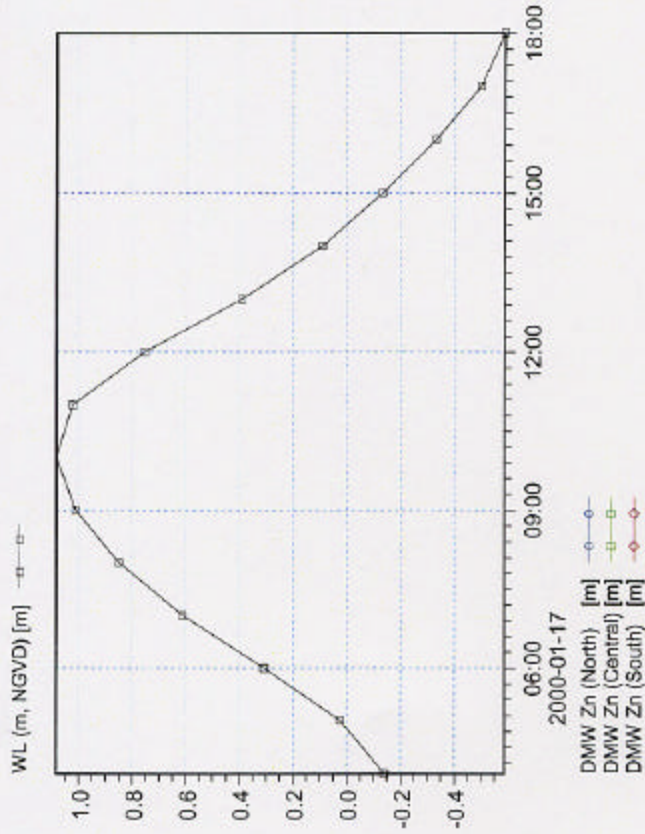
CASE 4 AVERAGE DISSOLVED ZINC (ug/L) IN THE REALIGNMENT (LEFT), WATER LEVEL (m) AND TIME SERIES OF ZINC (ug/L) (RIGHT)


Drawing no.

FIG. E2-10d



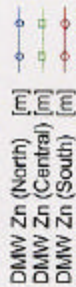
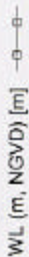
CASE 5: MAX Zn IN REALIGNMENT SEDIMENT



		Client:	RHODIA MARTINEZ	
		Project:	REMEDIAL DESIGN REPORT PEYTON SLOUGH	
Date:	03/02	CASE 5 AVERAGE DISSOLVED ZINC (ug/L) IN THE REALIGNMENT (LEFT), WATER LEVEL (m) AND TIME SERIES OF ZINC (ug/L) (RIGHT)		Drawing no. FIG. E2-10e
Init:	BB			

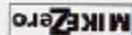
D:\RhodiaData\newymw\Rhodia\Rhodia\Figure5.dwg

D:\RhodiaData\newymw\Rhodia\Rhodia\Figure5.dwg



Downloaded from [www.jstor.org/stable/1121111](http://www.jstor.org/stable/1121111) by University of Chicago on Tue, 20 Jun 2017 12:00:00 UTC

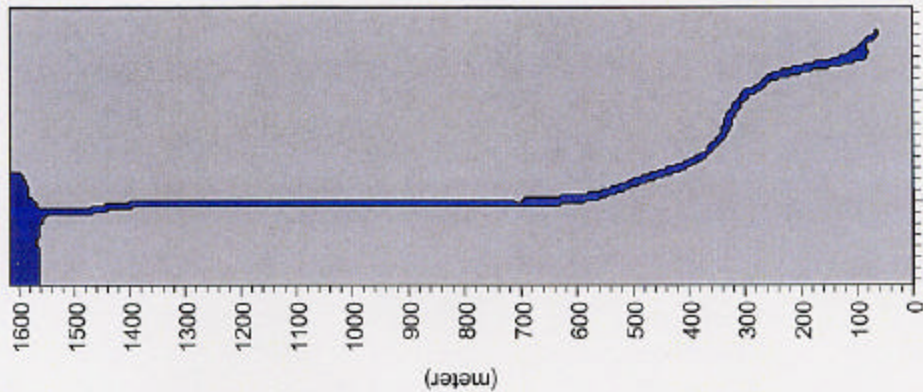
DOI: 10.1002/ajb.b.10001



REMEDIAL DESIGN REPORT PEYTON SLOUGH

Drawing no.

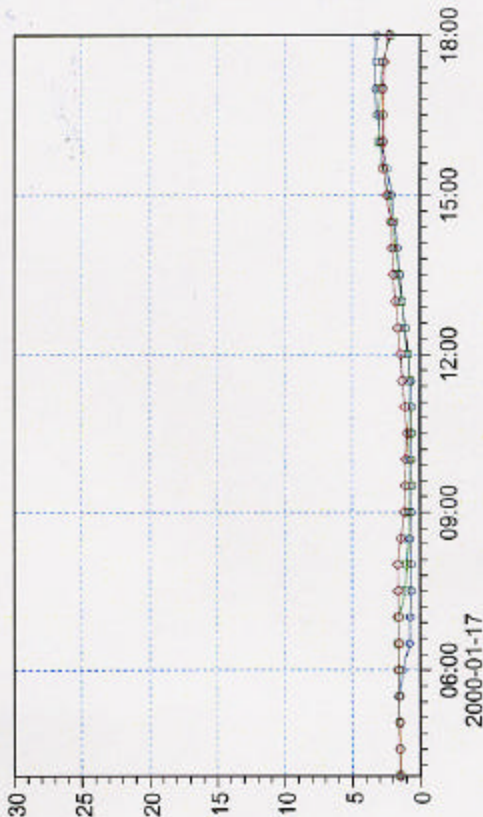
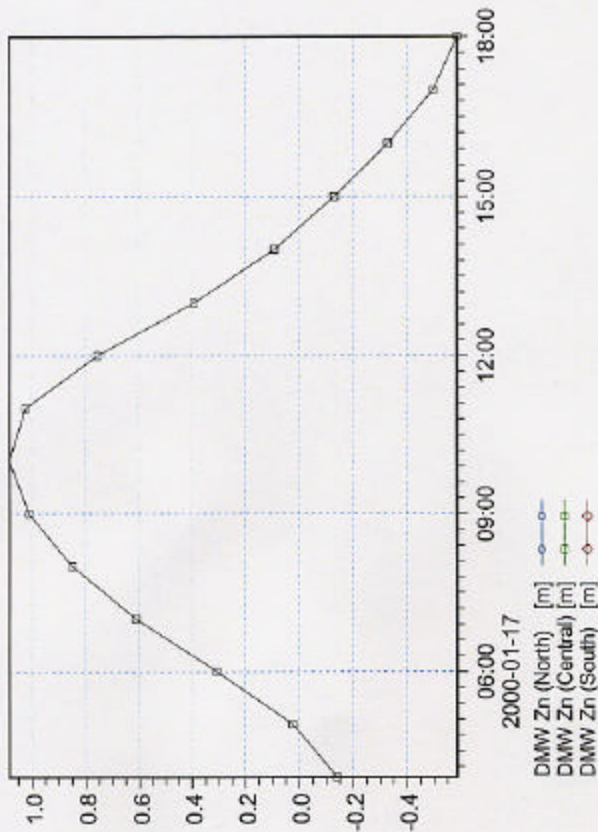
FIG. E2-10f



CASE 7: CASE 6 WITHOUT MVSD DISCHARGE



WL (m, NGVD) [m] —□—□—



<div> <div>URS</div> <div>Client: RHODIA MARTINEZ</div> </div>		<div> <div>MIKE2.0</div> <div>Project: REMEDIAL DESIGN REPORT PEYTON SLOUGH</div> </div>	
Date: 03/02	Init: BB	<div> <div>CASE 7 AVERAGE DISSOLVED ZINC (ug/L) IN THE REALIGNMENT (LEFT), WATER LEVEL (m) AND TIME SERIES OF ZINC (ug/L) (RIGHT)</div> <div>Drawing no. FIG. E2-10g</div> </div>	

D:\RhodiaData\heavy\mea\Result\FINAL FIGURE\W\_L\_Fig02-10g.dwg

D:\RhodiaData\heavy\mea\Result\FINAL FIGURE\W\_L\_Fig02-10g.dwg

**TABLE E-3-1 Summary of Surface Exchange Reactions Used in PHRREQC Runs**

Surface Type	Reaction	Log K	Reference
Clay	$X^- = X^-$	0	Appelo et al. 1998
	$Na^+ + X^- = NaX$	0	Appelo et al. 1998
	$Mg^{+2} + 2X^- = MgX_2$	0.8	Appelo et al. 1998
	$Ca^{+2} + 2X^- = CaX_2$	1.1	Appelo et al. 1998
	$Cu^{+2} + 2X^- = CuX_2$	0.9	See text
	$Zn^{+2} + 2X^- = ZnX_2$	1.1	See text
Organic Matter	$Y_a^- = Y_a^-$	0	Appelo et al. 1998
	$Na^+ + Y_a^- = NaY_a$	-1	Appelo et al. 1998
	$K^+ + Y_a^- = KY_a$	-0.75	Appelo et al. 1998
	$Mg^{+2} + 2Y_a^- = MgY_a_2$	-0.2	Appelo et al. 1998
	$Ca^{+2} + 2Y_a^- = CaY_a_2$	0.1	Appelo et al. 1998
	$Cu^{+2} + 2Y_a^- = CuY_a_2$	1.6	See text
	$Zn^{+2} + 2Y_a^- = ZnY_a_2$	1	See text
	$H^+ + Y_a^- = HY_a$	1.65	Appelo et al. 1998
	$Y_b^- = Y_b^-$	0	Appelo et al. 1998
	$H^+ + Y_b^- = HY_b$	3.3	Appelo et al. 1998
	$Y_c^- = Y_c^-$	0	Appelo et al. 1998
	$H^+ + Y_c^- = HY_c$	4.95	Appelo et al. 1998
	$Y_d^- = Y_d^-$	0	Appelo et al. 1998
	$H^+ + Y_d^- = HY_d$	6.85	Appelo et al. 1998
	$Y_e^- = Y_e^-$	0	Appelo et al. 1998
	$H^+ + Y_e^- = HY_e$	9.6	Appelo et al. 1998
	$Y_f^- = Y_f^-$	0	Appelo et al. 1998
	$H^+ + Y_f^- = HY_f$	12.35	Appelo et al. 1998
Amorphous iron	$Z = Z$	0	Appelo et al. 1998
	$H^+ + OH^- + Z = H_2OZ$	0	Appelo et al. 1998
	$H^+ + HCO_3^- + Z = H_2CO_3Z$	-3.3	Appelo et al. 1998
	$H^+ + ClO_4^- + Z = HClO_4Z$	-7.05	Appelo et al. 1998

**TABLE E-3-2. Summary of Input Parameters Used in PHREEQC Runs**

Parameter Type	Parameter	GRD 5	GRD 1	MW 25	MW 20	UNITS
Aqueous	Temp <sup>1</sup>	16	16	16	16	(deg. C)
	pH <sup>1</sup>	4.8	7.1	4.5	6.7	
	pe <sup>2</sup>	1.64E+01	1.41E+01	4.07E-01	-2.86E+00	
	Ca <sup>3</sup>	5.40E+02	9.80E+02	1.30E+03	6.60E+02	(ppm)
	Mg <sup>3</sup>	5.40E+02	9.80E+02	1.30E+03	6.60E+02	(ppm)
	Na <sup>4</sup>	4.61E+02	8.61E+02	6.46E+02	5.23E+02	(ppm)
	K <sup>4</sup>	1.71E+01	3.19E+01	2.39E+01	1.94E+01	(ppm)
	Fe <sup>5</sup>	9.00E-02	9.00E-02	9.00E-02	9.00E-02	(ppm)
	Mn <sup>4</sup>	8.57E-06	1.60E-05	1.20E-05	9.71E-06	(ppm)
	Si <sup>4</sup>	1.83E-01	3.42E-01	2.57E-01	2.08E-01	(ppm)
	Cl <sup>4</sup>	8.29E+02	1.55E+03	1.16E+03	9.40E+02	(ppm)
	Alkalinity <sup>3</sup>	1.62E+03	2.94E+03	3.90E+03	1.98E+03	(ppm)
	SO <sub>4</sub> <sup>1</sup>	1.80E+03	9.70E+02	5.00E+03	1.90E+02	(ppm)
	N(5) <sup>6</sup>	1.00E+00	1.00E+00	1.00E+00	1.00E+00	(ppm)
	N(-3) <sup>6</sup>	1.20E+01	1.20E+01	1.20E+01	1.20E+01	(ppm)
	O(0) <sup>1,7</sup>	2.10E+00	2.30E+00	4.00E-05	4.00E-05	(ppm)
	As <sup>5</sup>	2.50E-03	2.50E-03	2.50E-03	2.50E-03	(ppm)
	Cd <sup>5</sup>	5.00E-04	5.00E-04	5.00E-04	5.00E-04	(ppm)
	Cu <sup>1</sup>	9.30E+00	1.70E-02	1.70E-01	6.90E-03	(ppm)
	Pb <sup>5</sup>	1.80E-03	1.80E-03	1.80E-03	1.80E-03	(ppm)
	Ni <sup>5</sup>	2.50E-03	2.50E-03	2.50E-03	2.50E-03	(ppm)
	Zn <sup>1</sup>	2.50E+01	5.00E-02	2.70E+01	5.70E-02	(ppm)
	L(1) <sup>8</sup>	3.68E-05	5.01E-05	1.07E-07	4.60E-07	(molal)
	L(2) <sup>8</sup>	1.98E-04	2.70E-04	5.78E-07	2.48E-06	(molal)
Surface	X <sup>9</sup>	2.97E+00	2.97E+00	2.97E+00	2.97E+00	(moles)
	Ya <sup>9</sup>	2.47E-01	2.47E-01	2.47E-01	2.47E-01	(moles)
	Yb <sup>9</sup>	2.47E-01	2.47E-01	2.47E-01	2.47E-01	(moles)
	Yc <sup>9</sup>	2.47E-01	2.47E-01	2.47E-01	2.47E-01	(moles)
	Yd <sup>9</sup>	2.47E-01	2.47E-01	2.47E-01	2.47E-01	(moles)
	Ye <sup>9</sup>	2.47E-01	2.47E-01	2.47E-01	2.47E-01	(moles)
	Yf <sup>9</sup>	2.47E-01	2.47E-01	2.47E-01	2.47E-01	(moles)
	Z <sup>9</sup>	3.32E-03	3.32E-03	3.32E-03	3.32E-03	(moles)

<sup>1</sup>Measured; <sup>2</sup>Calculated from measured concentrations of redox sensitive aqueous species; <sup>3</sup>Calculated from molar fraction of measured hardness

<sup>4</sup>Calculated from measured salinity and relative amount of sodium in saline water (Nordstrom et al., 1979); <sup>5</sup>From long-term monitoring wells;

<sup>6</sup>Average concentrations in soil (Stumm and Morgan, 1996); <sup>7</sup>For reduced fluids set to pe; <sup>8</sup>Calculated from Donat et al. (1994) (see text);

<sup>9</sup>Calculated from physical and chemical properties of soil and equations given in Appelo et al. (1998);

## **Appendix E-3. Surface and Aqueous Speciation Model**

### **E-3-1 Model Description**

In order to gain an understanding of contaminant mobility at the project site, speciation calculations were performed using the PHREEQC modeling software (Parkhurst and Appelo, 1999). This software uses a thermodynamic database (Allison et al., 1990) and a chemical description of solid and aqueous phases determined through laboratory analysis to predict the distribution of each element in solid, surface, aqueous, and gaseous phases. PHREEQC is based on chemical thermodynamics and the energetics of possible chemical reactions are supplied to the program through the thermodynamic database. PHREEQC uses this information, along with the total elemental compositions of the system being modeled, to minimize the overall energy of the system. PHREEQC simultaneously solves expressions relating the mass of each element to the possible distribution of the element between different forms (mass balance equations), expressions representing the Gibbs free energy change of prescribed reactions (mass action equations), and an expression for electrical neutrality of the system (the charge balance equation).

### **E-3-2 Processes Modeled**

#### **Introduction**

PHREEQC models several types of chemical processes: aqueous phase reactions; ion exchange; surface complexation; and precipitation/dissolution. The first of these, homogenous aqueous reactions, are chemical reactions which occur between dissolved species. By contrast, ion exchange reactions are heterogenous adsorption/desorption processes normally associated with interactions between dissolved species and phases with fixed charges (i.e. clay minerals (Deutsch, 1997)). Surface complexation reactions, another type of adsorption/desorption process, are characterized by aqueous species attaching themselves via chemical bonds to functional groups present on the surface of sorbing phases. Finally, precipitation and dissolution are processes where aqueous species are irreversibly transformed to or from the solid phase, respectively.

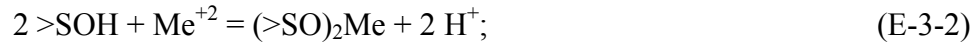
#### **Aqueous Reactions**

The primary modification to the thermodynamic database required to model the project site was the inclusion of equilibrium constants for copper sulfide complexes (Mountain and Seward, 1999) and organic ligands. The organic speciation of copper and zinc is difficult to quantify because there are many different possible organic ligands in natural systems. To overcome this challenge, chemists have identified classes of organic ligands and have subsequently measured their collective stability constants (Coale and Bruland, 1988; Donat et al., 1994; Zamzow et al., 1998; Bruland et al., 2000). The stronger ligand class is called  $L_1$  and may be related to phytoplankton (Coale and Bruland, 1988), EDTA release (Sedlak et al., 1997), or for this study, porewater biological processes (Skrabal et al., 1997). The weaker ligand is termed  $L_2$ , and is presumed to be composed of humic and fulvic substances (Coale and Bruland, 1988).

This study used the stability constants measured by Donat et al. (1994), and assumed a linear relationship between DOC and the relative quantity of the L<sub>1</sub> and L<sub>2</sub> ligands. For zinc, stability constants for L<sub>1</sub> and L<sub>2</sub> ligands have not been measured, therefore they were estimated from the constants for copper based on relative affinity for humic substances (Mantoura et al., 1977).

### **Adsorption and Desorption Processes**

Copper and zinc adsorb to clay particles because there is an electrostatic attraction between positively charged ions and negatively charged surface interfaces. The surface charge on clays results from two processes: 1) ionic substitution of Al<sup>+3</sup> for Si<sup>+4</sup> in the crystal lattice (ion exchange); and 2) the ionization of aluminol and silanol hydroxide functional groups at crystal edges (surface complexation) (Stumm and Morgan, 1996). In the former case, major cations in solution adsorb onto the internal and external surface area of the particles to neutralize the charge. Trace metals such as copper and zinc then compete with the major cations through a process of replacement (or ion exchange). In the latter process (surface complexation), trace metals compete with H<sup>+</sup> ions and other cations to form surface complexes with oxygen atoms:



where [ $>\text{S}$ ] denotes the mineral surface. This surface complexation process is pH dependent. As pH increases, an adsorption edge is observed in laboratory experiments where trace metals more effectively compete for the surface hydroxyl groups.

Ion exchange is normally modeled by assuming that all exchange sites in the mineral are occupied (Appelo and Postma, 1993). There is thus no net surface charge, and after the number of exchange sites has been defined, equilibria can be calculated from a set of exchange constants using mass action, mass balance, and charge balance equations.

Surface complexation processes are more difficult to model because surface sites can have net surface charges that must be balanced within a diffuse region extending into the solution (Adamson, 1990). Because the dielectric permittivity of this diffuse region is necessarily different than the bulk medium, the electrical potential energy of an ion in the vicinity of a charged surface is also modified. Consequently, the reactivity of the ion changes, and surface equilibrium constants must be corrected for surface charge (Koretsky, 2000). The constant capacitance model, the diffuse double layer model, and the triple layer model are three methods for correcting for changes in the vicinity of a surface (Schindler and Stumm, 1987).

Due to the fact that the database for all possible surface reactions is currently incomplete, and because there is uncertainty about the type and number of surface sites in sediment, two simplifications have been employed to successfully model natural systems. The first is the use of empirical surface complexation constants derived specifically for the sediment of interest (Davis et al., 1998; Celis, et al., 2000). The second is the use of a non-electrostatic model (James and Parks, 1975; Davis et al., 1987). This latter approach has been shown to be viable because the chemical contribution to the Gibbs free energy of adsorption is much larger than the electrostatic contribution for moderately or strongly sorbing ions such as copper and zinc.

This study used the empirical exchange constants derived by Appelo et al. (1998) for a non-electrostatic model of pyrite oxidation of marine sediment. Besides being similar to the processes of interest in this study, the model of Appelo et al. (1998) was deemed suitable because

relationships were derived between surface properties of the sediment and basic soil properties such as grain size, organic content, porosity, and bulk density. Although exchange constants for copper and zinc were not included in the database, exchange was estimated from the relative ratio of constants provided in consistent thermodynamic databases for montmorillonite (Fletcher and Sposito, 1989) and humic substances (Tipping and Hurley, 1992).

### **Precipitation and Dissolution Processes**

The complete thermodynamic database of Allison et al. (1990) was used in PHREEQC model runs. During the initial speciation runs, no solid phases were allowed to precipitate. Instead, saturation indices were reported for iron, sulfur, copper, zinc, and calcium-bearing phases. These saturation indices are a relative indicator of the propensity of the solution to precipitate a given mineral. Values greater than 0 indicate that a solution can lower its thermodynamic potential through precipitation. During model runs where precipitation was allowed to occur, all of the minerals in the table were free to precipitate if supersaturated. To incorporate the neutralization capacity of the soil, dissolution of montmorillonite clay was also allowed to occur (the pH neutralization capacity of clay was low).

### **E-3-3 Model Input**

Surface complexation reaction constants for model runs are listed in Table E-3-1. Corresponding elemental and surface input parameters are reported in Table E-3-2. Assumptions inherent in estimating elemental composition are listed in the footnotes.

### **E-3-4 Model Uncertainty**

There was no calibration of the model other than the calibration performed by Appelo et al. (1998). A proper calibration would require mineralogic and surface characterization of the sediment, and a complete water analysis. Also, because the model of Appelo et al. (1998) would undoubtedly produce at least modest differences in predictions than those using measured surface properties from the project site, initial estimates of surface and organic complexation constants shown on Table X-1 would need to be refined.

Based on limited information on the surface and aqueous chemistry of the project site, contaminant mobility was only assessed qualitatively in this study. For global processes described in Section 3.5.4, it is asserted that this is a proper use of the PHREEQC model. Chemical processes inferred from the model are not only consistent with spatial and temporal trends in deep and shallow groundwater monitoring wells, but also predicted the stability of mineral phases observed in the vicinity of sulfidic waste (Blowes and Jambor, 1990).

#### **Appendix E-4**

##### **Calculation of Mass Loading to New Alignment**

The mass loading of copper and zinc into the new alignment was calculated as the flow rate into the channel times the concentration:

$$L_x = C_x * Q \quad (E-4.1)$$

Where:

$L_x$  = is the loading rate of copper or zinc in grams

$C_x$  = is the concentration of copper or zinc in groundwater seeping into the channel

$Q$  = is the seepage rate into the new channel

$Q$  is the seepage rate in cubic feet /year/feet<sup>2</sup>

Which equals 0.16 ft<sup>3</sup>/year/ft<sup>2</sup>

See section 3.4 and 3.5.3 for source of seepage rate

Exhibit E-4-1 shows the results of calculations using Equation E-4.1. The concentrations for copper and zinc for each location are described in Section 3.5.2.

<b>Exhibit E-4-1</b>				
<b>Mass Loading into the New Alignment</b>				
<b>Location</b>	<b>Concentrations (mg/L)</b>		<b>Mass Flux into Channel (mg/day/ft<sup>2</sup>)</b>	
	<b>Cu</b>	<b>Zn</b>	<b>Cu</b>	<b>Zn</b>
North of Levee	0.005	0.036	6.26E-05	4.51E-04
Drainage Ditch	0.027	0.145	3.38E-04	1.82E-03
South of Levee (background)	0.01	0.038	1.25E-04	4.76E-04
South of Levee (ERMs)	0.014	0.05	1.75E-04	6.26E-04

#### **Mass Contributed by Tides**

Mass loading from the tides was calculated using Equation E-4.1 with  $Q$  equal to the tidal prism in cubic feet. The tidal prism was obtained from the calculations described in Section 3.4, Channel Design. The average tidal prism (i.e., the volume of water that enters the channel during an average tide) was estimated to be:

$$Tp = \text{tidal prism (cubic feet)} = 1,835,048$$

The concentration of copper in the north bay from the RMP data is 0.0019 mg/L. The concentration of zinc is 0.0008 mg/L.

The mass of copper or zinc contributed by the bay is then:

Mass of copper =  $TP \times 0.0019 = 98.6g$

Mass of zinc =  $TP \times 0.0008 = 41.5g$

### Mass Contributed by Groundwater

The mass contributed by groundwater is the flux rate from Exhibit E-4-1 times the surface area of the channel contributing groundwater to the channel times the length of time to seepage occurs. The surface area was calculated as the length of the channel times the depth times 2. The 2 accounts for seepage occurring on both sides of the channel. Exhibit E-4-2 shows the data used in the analysis.

<b>Exhibit E-4-2 Channel Data Used to Calculate Groundwater Seepage (feet)</b>	
Length of channel North of Levee	2800
Depth North of Levee	6.5
Length of Channel South of Levee that is 4.5 feet deep	1300
Length of Channel South of Levee that is 3.5 feet deep	1100
Length of Drainage Ditch near Spoil Piles	500
Depth of Drainage Ditch	6.5

The mass of copper and zinc seeping into the channel north of the levee during an ebb tide is the mass that seeps into the entire channel length for an complete tide cycle, or 12 hours. This is because groundwater will seep into the channel during the incoming tide (i.e., flood tide), then additional copper and zinc will seep into the channel as the same waters leaves during the ebb tide.

$$\text{Mass}_{gw} = \Sigma q * L * D * \text{Duration} * 2$$

$\text{Mass}_{gw}$  = mass of the copper and zinc seeping into channel (g)

$\Sigma$  = sum over all the channels contributing groundwater (i.e., channel north of the levee, channel south of the levee, drainage ditch)

$q$  = Mass flux into channel (mg/day/ft<sup>2</sup>) from Exhibit E-4-1.

$L$  = Length of the channel (feet)

$D$  = Depth of the channel (feet)

Duration = Length of tide (12 hours for Ebb 4.75 for Flood)

2 = Accounts for both sides of the channel

The mass that seeps into the channel from groundwater is dependent upon the concentration in the fill used for remediation south of the levee. Two assumption were made. If the fill has a concentration equal to background levels (See Section 3.5.2.1 for description of how background concentrations were determined) the mass of copper and zinc seeping into the channel during ebb tide is shown in Exhibit E-4-3.

**Exhibit E-4-3 Mass of Copper and Zinc seeping into Channel North of Levee During Ebb Tide (outgoing tide)**

Location	Concentrations		Mass Flux into Channel (mg/day/ft <sup>2</sup> )		Mass of Groundwater seeping into Channel (g)	
	Cu (mg/L)	Zn	Cu	Zn	Cu	Zn
North of Levee	0.005	0.036	6.26E-05	4.51E-04	3.45E-03	1.87E-02
Drainage Ditch	0.027	0.145	3.38E-04	1.82E-03	1.10E-03	5.90E-03
South of Levee (background)	0.01	0.038	1.25E-04	4.76E-04	1.21E-03	4.62E-03

If the fill has a concentration equal to ERMs the mass of copper and zinc seeping into the channel during ebb tide is shown in Exhibit E-4-4.

**Exhibit E-4-4 Mass of Copper and Zinc seeping into Channel North of Levee During Ebb Tide (outgoing tide)**

Location	Concentrations		Mass Flux into Channel (mg/day/ft <sup>2</sup> )		Mass of Groundwater seeping into Channel (g)	
	Cu	Zn	Cu	Zn	Cu	Zn
North of Levee	0.005	0.036	6.26E-05	4.51E-04	4.84E-03	2.02E-02
Drainage Ditch	0.027	0.145	3.38E-04	1.82E-03	1.35E-03	5.90E-03
South of Levee (ERMs)	0.014	0.05	1.75E-04	6.26E-04	2.09E-03	6.07E-03

During flood tide the mass of copper and zinc seeping into the channel is the amount that seeps into the channel during the rising tide which lasts about 4.75 hours. During flood tide groundwater that seeps into the channel south of the levee does not enter the channel north of the levee until ebb tide so was not included in the calculations.

**Exhibit E-4-5 Mass of Copper and Zinc seeping into Channel North of Levee During Flood Tide (incoming tide)**

Location	Concentrations (mg/L)		Mass Flux into Channel (mg/day/ft)		Mass of Groundwater seeping into Channel (g)	
	Cu	Zn	Cu	Zn	Cu	Zn
North of Levee	0.005	0.036	6.26E-05	4.51E-04	8.86E-04	5.58E-03
Drainage Ditch	0.027	0.145	3.38E-04	1.82E-03	4.35E-04	2.34E-03

